SUPPORTING INFORMATION

Photoefficient 2nd Generation Molecular Motors Responsive to Visible Light

Lukas Pfeifer, Maximilian Scherübl, Maximilian Fellert, Wojciech Danowski, Jinling Cheng, Jasper Pol, Ben L. Feringa

Stratingh Institute for Chemistry, University of Groningen, Nijenborgh 4, 9747 AG Groningen, The Netherlands

Table of Contents

1. General Information

Reagents were purchased from Sigma Aldrich, Acros or TCI Europe and were used as received. Nematic E7 liquid crystal mixture (average molecular weight: 274 g/mol) was purchased from Merck Japan Ltd. Solvents were reagent grade and used without prior water removal unless otherwise indicated. Anhydrous solvents were obtained from an MBraun SPS-800 solvent purification system or directly bought from Acros. Solvents were degassed by purging with N_2 for a minimum of 30 min or by three freeze-pump-thaw cycles.

Flash column chromatography was performed on silica gel (Merck, type 9385, 230–400 mesh) or on a Büchi Reveleris purification system using Büchi silica cartridges. Thin layer chromatography was carried out on aluminium sheets coated with silica gel 60 F254 (Merck). Compounds were visualized with a UV lamp and/or by staining with $KMnO_4$, CAM or vanillin.

^1H and ^{13}C NMR spectra were recorded on a Varian Mercury-Plus 400 or a Bruker Avance 600 NMR spectrometer at 298 K unless otherwise indicated. PSS studies were performed on a Varian Unity Plus 500 NMR spectrometer. Chemical shifts are given in parts per million (ppm) relative to the residual solvent signal. Multiplets in ^1H NMR spectra are designated as follows: s (singlet), d (doublet), t (triplet), q (quartet), p (pentet), m (multiplet), br (broad). High resolution mass spectrometry (ESI) was performed on an LTQ Orbitrap XL spectrometer. UV-vis absorption spectra were recorded on an Agilent 8453 UV-vis Diode Array System, equipped with a Quantum Northwest Peltier controller, in 10 mm quartz cuvettes. Irradiation experiments were performed using fiber-coupled LEDs (M420F2, M455F1, M470F3, M490F3, M505F3, M530F2) obtained from Thorlabs Inc.. CD spectra were recorded on a Jasco J-810 CD spectrometer. Supercritical fluid chromatography (SFC) was performed on a Thar Technologies Inc. SFC (Waters) system, equipped with fluid delivery module (FDM10-1), an autosampler (a modified Alias 840), a semi-prep column oven, PDA detector, a back pressure regulator (ABPR20), heat-exchanger, and a fraction collector (modified Thar SFC-FC). Liquid crystals were studied using a LV100NPOL polarized microscope, purchased from Nikon equipped with a Nikon DS Fi-3 camera and a Microscope Hot-stage System HS82. NIS Elements D software was used for acquisition of images.

2. Preparation and Characterization of Compounds

2.1. Rotors

5-Methoxy-2-methyl-2,3-dihydro-1H-cyclopenta[a]naphthalen-1-one (S1)

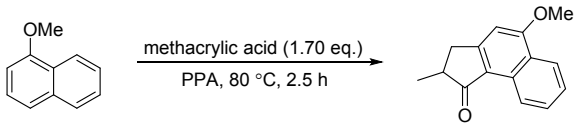

S1

A three-neck flask equipped with a mechanical stirrer was charged with polyphosphoric acid (PPA, 115% H_3PO_4, 80 mL), heated to 80 °C and 1-methoxynaphtalene (13.1 mL, 90.0 mmol) was added over 3 min. After 5 min methacrylic acid (13.0 mL, 153 mmol) was added over 3 min and the resulting mixture was stirred at 80 °C for 2.5 h. The dark red mixture was allowed to cool to room temperature and the reaction was quenched by adding ice. After stirring the mixture overnight it was extracted with EtOAc and the combined organic layers were dried over $MgSO_4$ and concentrated *in vacuo*. The crude product was purified *via* recrystallization from hot EtOH (250 mL) to obtain **S1** (14.94 g, 66.02 mmol, 73%) as a pale yellow solid. Data is in accordance with literature.[1]

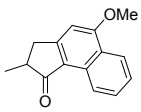

S1

^{1}H NMR (600 MHz, $CDCl_3$) δ 9.13 (d, J = 8.3 Hz, 1H), 8.25 (d, J = 8.4 Hz, 1H), 7.66 (ddd, J = 8.2, 7.0, 1.2 Hz, 1H), 7.52 (ddd, J = 8.3, 6.8, 1.3 Hz, 1H), 6.77 (s, 1H), 4.08 (s, 3H), 3.44 – 3.38 (m, 1H), 2.84 – 2.64 (m, 2H), 1.36 (d, J = 7.3 Hz, 3H); **^{13}C NMR** (151 MHz, $CDCl_3$) δ 208.5, 161.8, 159.3, 130.7, 129.4, 126.1, 125.3, 124.0, 123.6, 122.6, 101.6, 56.1, 42.3, 36.0, 17.0.

5-Bromo-2-methyl-2,3-dihydro-1H-cyclopenta[a]naphthalen-1-one (S2)

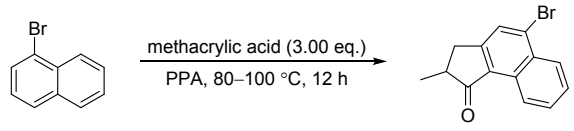

S2

A round-bottom flask was charged with polyphosphoric acid (PPA, 115% H_3PO_4, 50 mL) and warmed to 80 °C under mechanical stirring. 1-Bromonaphthalene (10.3 mL, 73.4 mmol) was added and the mixture stirred for 10 min before adding methacrylic acid (18.7 mL, 220 mmol). The reaction mixture was then warmed to 100 °C and left to stir for 12 h, before cooling to 50 °C and quenching with ice. After stirring for 2 h it was extracted with Et_2O, the combined organic layers were dried over Na_2SO_4 and solvents were removed *in vacuo*. Flash column chromatography (SiO_2, dry load on celite, 40–80% toluene in pentane) followed by recrystallization from hot heptane gave **S2** (1.16 g, 4.22 mmol, 5.7%) as an off-white solid. Data is in accordance with literature.[2]

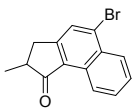

S2

^{1}H NMR (600 MHz, $CDCl_3$) δ 9.19 (d, J = 8.1 Hz, 1H), 8.30 (d, J = 8.4 Hz, 1H), 7.87 (s, 1H), 7.71 (ddd, J = 8.2, 7.0, 1.2 Hz, 1H), 7.65 (ddd, J = 8.3, 7.0, 1.2 Hz, 1H), 3.46 (dd, J = 18.0, 8.0 Hz, 1H), 2.83 – 2.79 (m, 2H), 1.38 (d, J = 7.3 Hz, 3H); **^{13}C NMR** (151 MHz, $CDCl_3$) δ 209.3, 156.4, 131.8, 131.3, 130.4, 130.0, 129.8, 128.5, 127.9, 127.7, 124.5, 42.7, 35.1, 16.7.

2.2. Stators

(3,6-Dimethoxy-9H-fluoren-9-ylidene)hydrazine (S7)

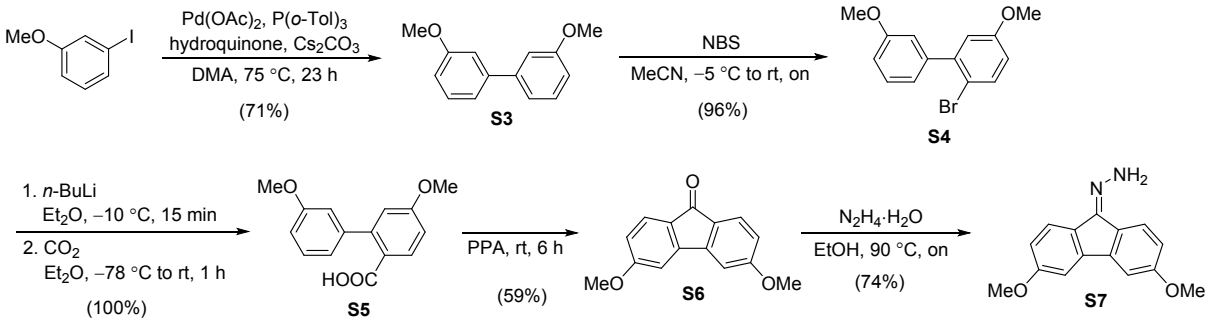

3,3'-Dimethoxy-1,1'-biphenyl (S3)

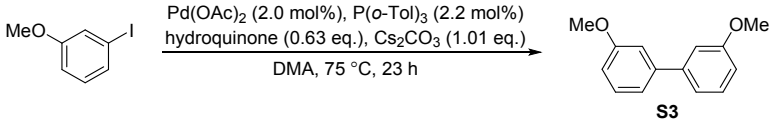

Anhydrous DMA (50 mL) was degassed in a Schlenk flask by purging with N_2 for 1 h. $Pd(OAc)_2$ (90 mg, 0.40 mmol) and P(*o*-tol)$_3$ (134 mg, 0.440 mmol) were added and the mixture was stirred until a homogeneous, yellow solution was formed. Hydroquinone (1.39 g, 12.6 mmol), Cs_2CO_3 (6.58 g, 20.2 mmol) and 3-iodoanisole (2.38 mL, 20.0 mmol) were added and the reaction mixture was stirred at 75 °C for 23 h. The reaction mixture was quenched with 2 M aq. HCl and subsequently extracted with EtOAc. The combined organic layers were washed with 0.1 M aq. NaOH solution and brine, dried over $MgSO_4$ and the solvent was evaporated *in vacuo*. The crude product was purified by flash column chromatography (SiO_2, dry load on celite, 3% Et_2O in pentane), giving **S3** (1.53 g, 7.14 mmol, 71%) as a colorless liquid crystallizing on standing. Data is in accordance with literature.[3]

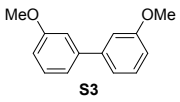

^{1}H NMR (400 MHz, $CDCl_3$) δ 7.36 (t, *J* = 7.9 Hz, 2H), 7.19 (dt, *J* = 7.6, 1.2 Hz, 2H), 7.13 (t, *J* = 2.1 Hz, 2H), 6.91 (dd, *J* = 8.2, 2.5 Hz, 2H), 3.87 (s, 6H); **^{13}C NMR** (151 MHz, $CDCl_3$) δ 160.0, 142.7, 129.8, 119.8, 113.1, 112.9, 55.3.

2-Bromo-3',5-dimethoxy-1,1'-biphenyl (S4)

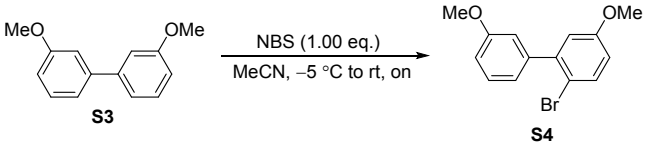

A Schlenk flask was charged with **S3** (1.98 g, 9.24 mmol) and anhydrous MeCN (20 mL) before the resulting solution was cooled down to –5 °C using a NaCl/H_2O/ice bath. In a second Schlenk flask *N*-bromosuccinimide (1.64 g, 9.24 mmol) was dissolved in anhydrous MeCN (20 mL). This solution was added dropwise over 1 h to the precooled solution of the substrate. The combined solutions were stirred at 0 °C for another 4 h, then warmed up to room temperature and stirred overnight. The reaction mixture was separated between H_2O and DCM and the aqueous layer was extracted with DCM. The combined organic layers were washed with 10% aq. Na_2SO_3 and brine, dried over $MgSO_4$ and solvents were evaporated *in vacuo*. The crude product was purified by flash column chromatography (SiO_2, dry load on celite, 11% DCM in pentane), giving **S4** (2.59 g, 8.83 mmol, 96%) as a colorless oil crystallizing on standing. Data is in accordance with literature.[4]

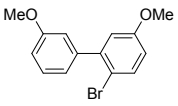

S4

^{1}H NMR (600 MHz, $CDCl_3$) δ 7.54 (d, J = 8.8 Hz, 1H), 7.34 (t, J = 7.9 Hz, 1H), 6.99 (dt, J = 7.5, 1.2 Hz, 1H), 6.97 – 6.92 (m, 2H), 6.89 (d, J = 3.1 Hz, 1H), 6.81 – 6.75 (m, 1H), 3.85 (s, 3H), 3.81 (s, 3H); **^{13}C NMR** (151 MHz, $CDCl_3$) δ 159.3, 158.9, 143.4, 142.6, 133.8, 129.1, 121.8, 116.7, 115.1, 114.9, 113.4, 113.1, 55.7, 55.4.

3',5-Dimethoxy-[1,1'-biphenyl]-2-carboxylic acid (S5)

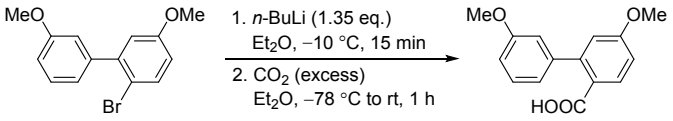

S4 **S5**

A Schlenk flask was charged with **S4** (2.00 g, 6.82 mmol) and anhydrous Et_2O (60 mL). The resulting solution was cooled to –10 °C using a $NaCl/H_2O$/ice bath and *n*-BuLi (2.5 M solution on hexanes, 3.68 mL, 9.21 mmol) was added dropwise. After 15 min a precipitate had formed and CO_2 was carefully bubbled through the reaction mixture while warming up to room temperature. Upon reaching full conversion as judged by TLC the mixture was acidified with 1 M aq. HCl. The product was extracted with Et_2O and the combined organic layers were washed with H_2O and brine and dried over $MgSO_4$. Solvent removal *in vacuo* gave **S5** (1.76 g, 6.81 mmol, 100%) as a waxy white solid which was subsequently used without further purification. Data is in accordance with literature.[5]

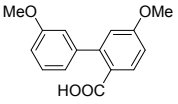

S5

^{1}H NMR (600 MHz, $CDCl_3$) δ 7.98 (d, J = 8.7 Hz, 1H), 7.28 (t, J = 7.8 Hz, 1H), 6.93 – 6.88 (m, 4H), 6.83 (d, J = 2.6 Hz, 1H), 3.86 (s, 3H), 3.81 (s, 3H); **^{13}C NMR** (151 MHz, $CDCl_3$) δ 172.4, 162.5, 159.2, 146.2, 142.9, 133.5, 129.0, 121.1, 119.8, 116.7, 114.2, 113.0, 112.8, 55.6, 55.4.

3,6-Dimethoxy-9H-fluoren-9-one (S6)

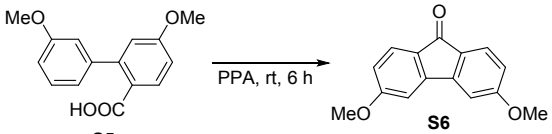

S5 **S6**

A three-necked flask was charged with polyphosphoric acid (115% H_3PO_4, 25 g) and equipped with a mechanical stirrer. Under continuous stirring, finely ground **S5** (1.76 g, 6.81 mmol) was added over 5 min. The reaction mixture was stirred for 6 h at room temperature before it was quenched by adding ice. After stirring at room temperature for 2 h the crude product was extracted with DCM, the organic layers were dried over $MgSO_4$ and solvents were removed *in vacuo*. The crude product was purified by flash column chromatography (SiO_2, dry load on silica, 40–100% DCM in pentane), giving **S6** (963 mg, 4.01 mmol, 59%) as an orange solid. Data is in accordance with literature.[6]

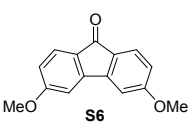

S6

^{1}H NMR (600 MHz, $CDCl_3$) δ 7.58 (d, J = 8.2 Hz, 2H), 6.99 (d, J = 2.2 Hz, 2H), 6.74 (dd, J = 8.2, 2.2 Hz, 2H), 3.90 (s, 6H); **^{13}C NMR** (151 MHz, $CDCl_3$) δ 191.5, 165.2, 146.0, 128.5, 125.9, 113.2, 107.2, 55.9.

(3,6-Dimethoxy-9H-fluoren-9-ylidene)hydrazine (S7)

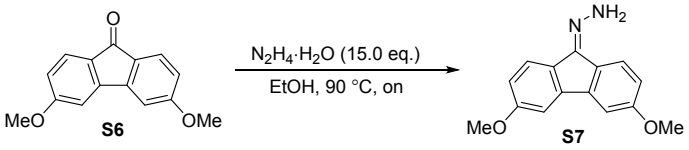

A flask was charged with ketone **S6** (240 mg, 1.00 mmol), EtOH and hydrazine monohydrate (50–60% in H_2O, 1.32 mL, 15.0 mmol). The reaction mixture was heated to 90 °C overnight leading to the formation of a yellow precipitate. After cooling to room temperature H_2O (2.0 mL) was added and the mixture was placed in a freezer (–25 °C) for 2 h, after which the solid product was filtered off. The solid was washed with cold H_2O/EtOH (1:1) and remaining H_2O was removed by co-evaporation with toluene to give **S7** (187 mg, 0.735 mmol, 74%) as a light-yellow solid. Data is in accordance with literature.[7] Note: The diazo derivative of **S7** is not stable and, therefore, has to be prepared immediately prior to the next step (*vide infra*).

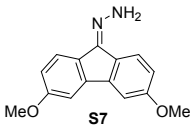

^{1}H NMR (600 MHz, $CDCl_3$) δ 7.86 (d, J = 8.4 Hz, 1H), 7.62 (d, J = 8.3 Hz, 1H), 7.23 (d, J = 2.4 Hz, 1H), 7.13 (d, J = 2.3 Hz, 1H), 6.86 (d, J = 2.2 Hz, 1H), 6.84 (d, J = 2.2 Hz, 1H), 6.09 (s, 2H), 3.92 (s, 3H), 3.89 (s, 3H); **^{13}C NMR** (151 MHz, $CDCl_3$) δ 161.2, 160.9, 146.2, 143.4, 140.1, 131.6, 127.0, 124.5, 122.0, 114.2, 112.9, 106.6, 105.1, 55.8, 55.7.

3,6-Dibromo-9-diazo-9H-fluorene (S10)

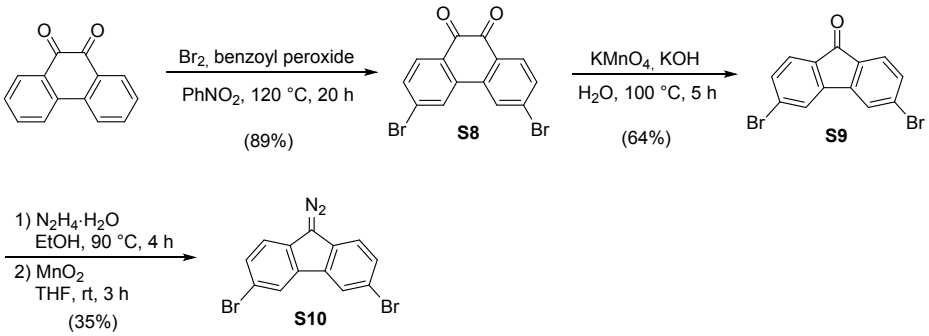

3,6-Dibromophenanthrene-9,10-dione (S8)

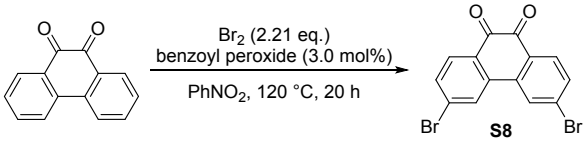

9,10-Phenanthrenedione (10.00 g, 48.03 mmol) and benzoyl peroxide (75 wt% in H_2O, 465 mg, 1.44 mmol) were dissolved in nitrobenzene (50 mL). Bromine (5.44 mL, 106 mmol) was added over 2 min under vigorous stirring. The mixture was heated to 120 °C for 20 h. After cooling to room temperature the formed precipitate was filtered off and washed with pentane. The mother liquor was concentrated *in vacuo* and filtered to give a second batch of product. **S8** (15.57 g, 42.54 mmol, 89%) was obtained as a yellow powder. Data is in accordance with literature.[2]

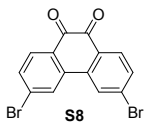

S8

^{1}H NMR (600 MHz, $CDCl_3$) δ 8.12 (d, J = 1.7 Hz, 2H), 8.07 (d, J = 8.3 Hz, 2H), 7.67 (dd, J = 8.3, 1.7 Hz, 2H); **^{13}C NMR** (151 MHz, $CDCl_3$) δ 179.0, 136.1, 133.6, 132.2, 130.0, 127.5.

3,6-Dibromo-9H-fluoren-9-one (S9)

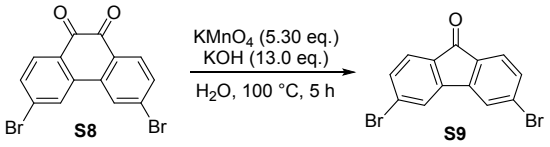

H_2O (58 mL) was added to a mixture of dibromophenanthrene **S8** (14.05 g, 38.39 mmol) and KOH (28.00 g, 499.0 mmol) and the mixture was heated to 100 °C. $KMnO_4$ (32.16 g, 203.5 mmol) was added portion wise over 2 h to the suspension and the final mixture was kept at 100 °C for additional 3 h. It was then allowed to cool to room temperature and conc. H_2SO_4 was added until neutral pH was obtained. Na_2SO_3 was added until the solution turned light yellow. The solid product was filtered off and after drying in an oven at 90 °C overnight product **S9** (8.27 g, 24.5 mmol, 64%) was obtained as a pale yellow solid. Data is in accordance with literature.[2]

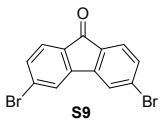

S9

^{1}H NMR (600 MHz, $CDCl_3$) δ 7.67 (d, J = 1.6 Hz, 2H), 7.55 (d, J = 7.8 Hz, 2H), 7.50 (dd, J = 7.8, 1.6 Hz, 2H); **^{13}C NMR** (151 MHz, $CDCl_3$) δ 191.5, 144.9, 133.0, 132.9, 130.0, 125.9, 124.3.

3,6-Dibromo-9-diazo-9H-fluorene (S10)

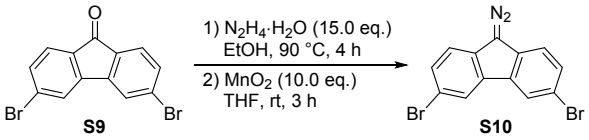

To a mixture of **S9** (3.00 g, 8.88 mmol) and absolute EtOH (90 mL) was added hydrazine monohydrate (50–60% in H_2O, 11.7 mL, 133 mmol) and the resulting light yellow suspension was heated to 90 °C. After 4 h the mixture was allowed to cool to room temperature and H_2O (10 mL) was added. The green suspension was put in the freezer at –25 °C to allow crystallization overnight. The solids were collected and a second batch was crystallized by adding water (15 mL) to the mother liquor and putting it in the freezer at –25 °C. The collection of both batches yielded a pale green solid as the corresponding hydrazone (1.94 g, 5.51 mmol, 62%). The crude hydrazone (1.67 g, 4.74 mmol) was dissolved in anhydrous THF (53 mL) and MnO_2 (4.12 g, 47.4 mmol) was added. The black suspension was stirred at room temperature for 3 h and then filtered over a plug of celite. The orange solution was concentrated *in vacuo* to yield product **S10** (946 mg, 2.70 mmol, 57%) as an orange solid. Note: This compound is not stable under ambient conditions for prolonged periods of time and should be stored at –20 °C. Data is in accordance with literature.[2]

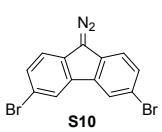

S10

^{1}H NMR (600 MHz, $CDCl_3$) δ 8.03 (s, 2H), 7.52 (d, J = 8.5 Hz, 2H), 7.37 (d, J = 8.2 Hz, 2H); **^{13}C NMR** (151 MHz, $CDCl_3$) δ 131.9, 131.8, 129.9, 124.5, 120.6, 118.4, 64.0.

2.3. Molecular Motors

1-(3,6-Dimethoxy-9H-fluoren-9-ylidene)-2-methyl-2,3-dihydro-1H-cyclopenta[a]naphthalene-5-carbonitrile (1_s)

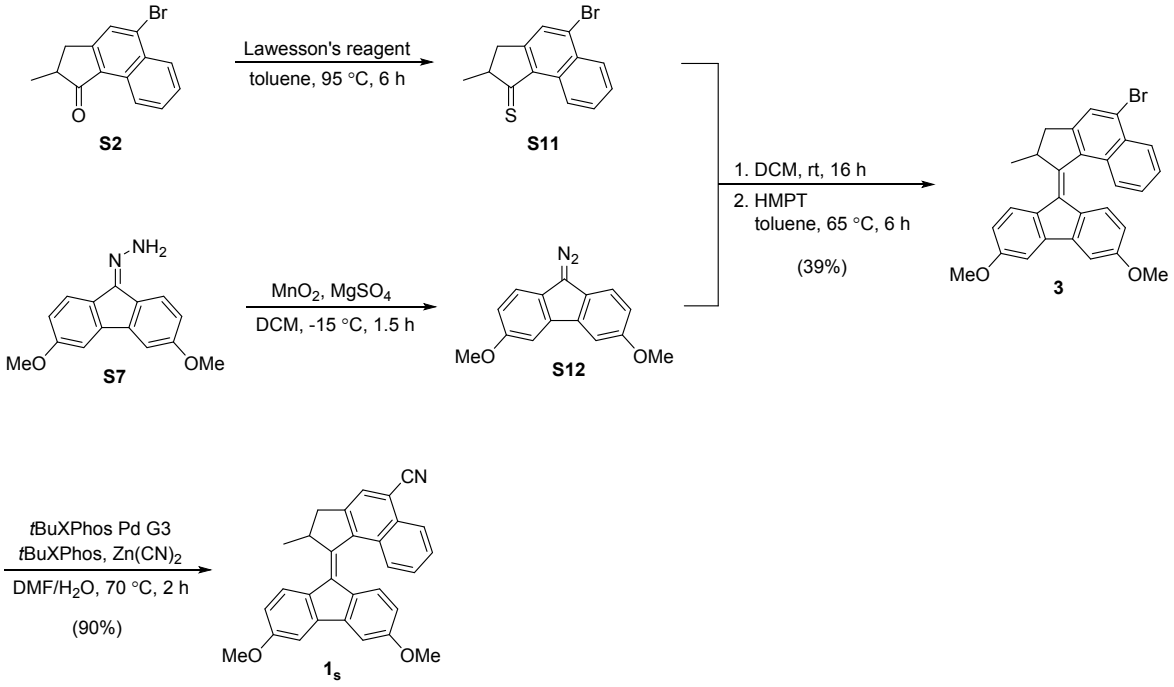

9-(5-Bromo-2-methyl-2,3-dihydro-1H-cyclopenta[a]naphthalen-1-ylidene)-3,6-dimethoxy-9H-fluorene (3)

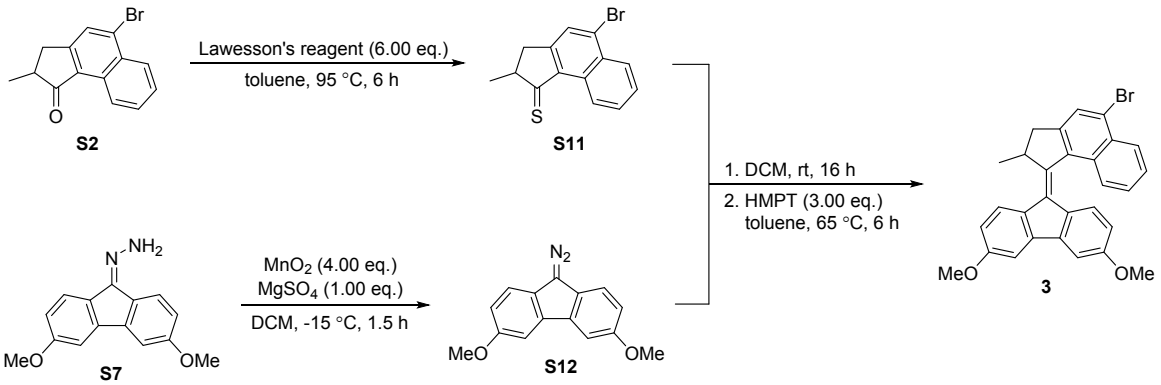

A mixture of ketone **S2** (55 mg, 0.20 mmol) and Lawesson's reagent (485 mg, 1.20 mmol) in anhydrous toluene (3.0 mL) was heated to 95 °C. After 6 h toluene was removed *in vacuo* and thioketone intermediate **S11** was purified by flash column chromatography (SiO_2, dry load on celite, 2–10% DCM in pentane). In parallel, a mixture of hydrazone **S7** (76 mg, 0.30 mmol), MnO_2 (104 mg, 1.20 mmol) and $MgSO_4$ (36 mg, 0.30 mmol) in anhydrous DCM (1.5 mL) was stirred at –15 °C for 1.5 h. The resulting suspension containing dissolved diazo intermediate **S12** was filtered over celite into a Schlenk flask. Thioketone dissolved in anhydrous DCM (750 µL) was added to this solution and the resulting mixture was stirred at room temperature for 16 h. Volatiles were removed *in vacuo*, the remaining solids were taken up in toluene (3.0 mL) and HMPT (109 µL, 0.600 mmol) was added. After stirring this mixture at 65 °C for 6 h volatiles were removed *in vacuo* and the desired product was purified by flash column chromatography (SiO_2, dry load on celite, 12–30% DCM in pentane). **3** (38 mg, 79 µmol, 39%) was obtained as a yellow solid.

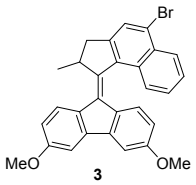

^{1}H NMR (600 MHz, $CDCl_3$) δ 8.36 (d, *J* = 8.5 Hz, 1H), 7.89 (s, 1H), 7.87 (s, 1H), 7.85 (s, 1H), 7.57 (ddd, *J* = 8.3, 6.8, 1.2 Hz, 1H), 7.37 (ddd, *J* = 8.2, 6.7, 1.2 Hz, 1H), 7.33 (d, *J* = 2.5 Hz, 1H), 7.23 (d, *J* = 2.5 Hz, 1H), 6.96 (dd, *J* = 8.5, 2.5 Hz, 1H), 6.59 (d, *J* = 8.7 Hz, 1H), 6.37 (dd, *J* = 8.7, 2.5 Hz, 1H), 4.25 (p, *J* = 6.6 Hz, 1H), 3.97 (s, 3H), 3.84 (s, 3H), 3.55 (dd, *J* = 15.0, 5.7 Hz, 1H), 2.70 (d, *J* = 15.1 Hz, 1H), 1.36 (d, *J* = 6.8 Hz, 3H); **^{13}C NMR** (151 MHz, $CDCl_3$) δ 159.6, 159.5, 146.8, 145.4, 141.7, 141.3, 137.1, 133.7, 131.2, 130.9, 130.7, 130.4, 128.4, 128.1, 127.9, 127.3, 127.0, 126.7, 125.2, 124.6, 113.5, 112.5, 104.9, 104.0, 55.8, 55.6, 45.2, 41.6, 19.4; **HRMS** (ESI pos) *m/z* calcd for $C_{29}H_{24}BrO_2$ $[M+H]^+$ 485.09337, found 485.09390.

1-(3,6-Dimethoxy-9H-fluoren-9-ylidene)-2-methyl-2,3-dihydro-1H-cyclopenta[a]naphthalene-5-carbonitrile (1_s)

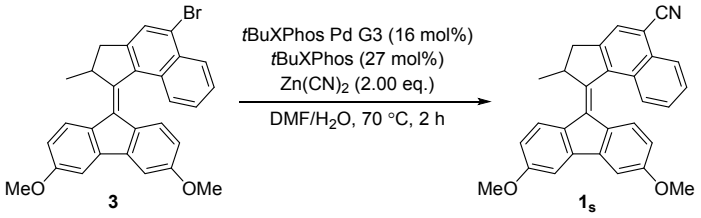

A N_2 filled Schlenk tube was charged with alkene **3** (25 mg, 52 µmol), *t*BuXPhos Pd G3 (6.6 mg, 8.3 µmol), *t*BuXPhos (5.9 mg, 14 µmol) and $Zn(CN)_2$ (12 mg, 0.10 mmol). A degassed (3x freeze-pump-thaw) mixture of DMF/H_2O (99:1, 900 µL) was added and the resulting solution was heated to 70 °C for 2 h. After cooling to room temperature the mixture was diluted with EtOAc, washed with brine, dried over $MgSO_4$ and concentrated *in vacuo*. The crude product was purified by flash column chromatography (SiO_2, dry load on celite, 10–35% DCM in pentane) to obtain the final compound **1_s** (20 mg, 47 µmol, 90%) as an orange solid.

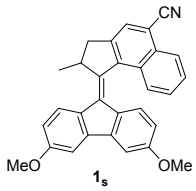

^{1}H NMR (600 MHz, $CDCl_3$) δ 8.33 (d, *J* = 8.3 Hz, 1H), 7.96 (s, 1H), 7.93 (d, *J* = 8.4 Hz, 1H), 7.83 (d, *J* = 8.6 Hz, 1H), 7.65 (ddd, *J* = 8.3, 6.8, 1.2 Hz, 1H), 7.42 (ddd, *J* = 8.3, 6.8, 1.2 Hz, 1H), 7.29 (d, *J* = 2.5 Hz, 1H), 7.19 (d, *J* = 2.5 Hz, 1H), 6.94 (dd, *J* = 8.5, 2.5 Hz, 1H), 6.51 (d, *J* = 8.7 Hz, 1H), 6.34 (dd, *J* = 8.7, 2.5 Hz, 1H), 4.26 (p, *J* = 6.7 Hz, 1H), 3.96 (s, 3H), 3.83 (s, 3H), 3.56 (dd, *J* = 15.1, 5.8 Hz, 1H), 2.75 (d, *J* = 15.1 Hz, 1H), 1.34 (d, *J* = 6.8 Hz, 3H); **^{13}C NMR** (151 MHz, $CDCl_3$) δ 160.2, 160.1, 144.8, 143.9, 142.8, 142.2, 141.8, 133.4, 133.1, 132.1, 130.9, 130.2, 129.4, 128.4, 127.9, 127.8, 127.1, 126.0, 125.61, 118.5, 113.6, 112.5, 110.6, 105.2, 104.4, 55.8, 55.6, 45.3, 41.4, 19.2; **HRMS** (ESI pos) *m/z* calcd for $C_{30}H_{24}NO_2$ $[M+H]^+$ 430.18016, found 430.17997.

9-(5-Methoxy-2-methyl-2,3-dihydro-1H-cyclopenta[a]naphthalen-1-ylidene)-9H-fluorene-3,6-dicarbonitrile (2_s)

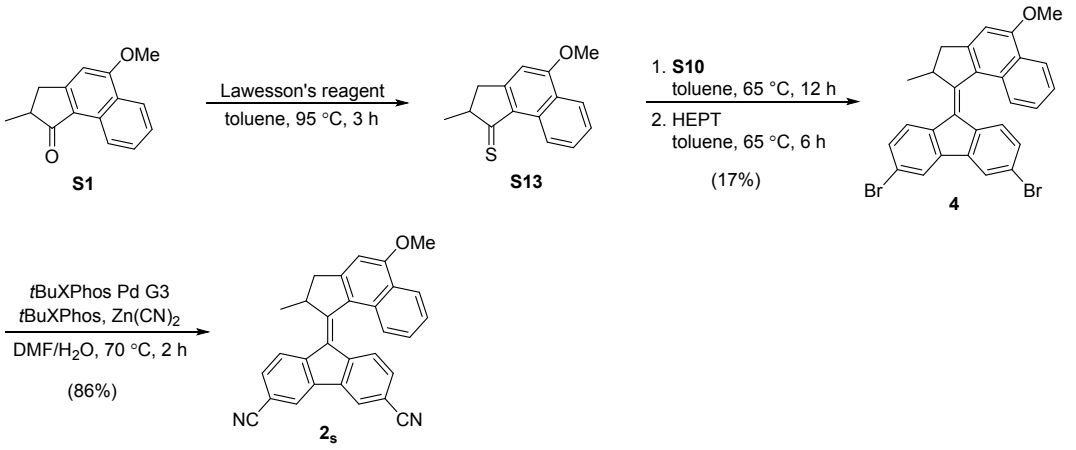

3,6-Dibromo-9-(5-methoxy-2-methyl-2,3-dihydro-1H-cyclopenta[a]naphthalen-1-ylidene)-9H-fluorene (4)

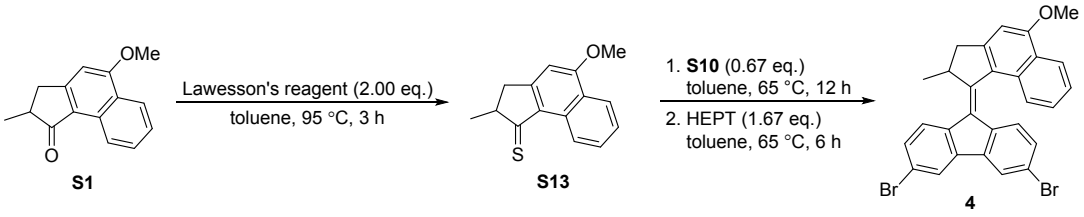

Ketone **S1** (500 mg, 2.21 mmol) and Lawesson's reagent (1.79 g, 4.42 mmol) were dissolved in anhydrous toluene (40 mL) and heated to 95 °C. After 3 h the color had changed from pale yellow to dark red and the solvent was removed *in vacuo*. The crude product was purified by flash column chromatography (SiO_2, dry load on celite, 6–7% EtOAc in pentane) giving thioketone **S13** as a red solid. The product was used immediately for the next step. Thioketone **S13** and diazo **S10** (516 mg, 1.47 mmol) were dissolved in anhydrous toluene (40 mL) and heated to 65 °C. After 12 h tris(diethylamino)phosphine (HEPT, 1.01 mL, 3.69 mmol) was added and the mixture was stirred at 65 °C for another 6 h. The red solution was concentrated *in vacuo* and purified by flash column chromatography (SiO_2, dry load on celite, 10–20% DCM in pentane). The desired product **4** (136 mg, 0.256 mmol, 17%) was obtained as an orange solid.

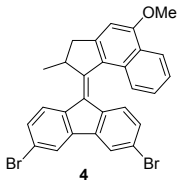

^{1}H NMR (600 MHz, $CDCl_3$) δ 8.36 (d, J = 8.0 Hz, 1H), 7.94 (d, J = 1.9 Hz, 1H), 7.85 (d, J = 1.9 Hz, 1H), 7.82 (d, J = 8.4 Hz, 1H), 7.59 (d, J = 8.4 Hz, 1H), 7.51 (dd, J = 8.3, 2.0 Hz, 1H), 7.47 (ddd, J = 8.2, 6.8, 1.2 Hz, 1H), 7.37 (ddd, J = 8.3, 6.8, 1.4 Hz, 1H), 6.96 (s, 1H), 6.94 (dd, J = 8.5, 1.9 Hz, 1H), 6.55 (d, J = 8.4 Hz, 1H), 4.23 (p, J = 6.6 Hz, 1H), 4.12 (s, 3H), 3.56 (dd, J = 15.1, 5.6 Hz, 1H), 2.75 (d, J = 15.1 Hz, 1H), 1.38 (d, J = 6.7 Hz, 3H). **^{13}C NMR** (151 MHz, $CDCl_3$) δ 158.7, 153.8, 150.2, 140.3, 139.8, 138.9, 136.2, 130.5, 130.2, 129.2, 128.1, 127.7, 127.1, 127.1, 126.4, 125.1, 125.1, 124.9, 123.1, 122.3, 120.4, 120.4, 102.7, 56.0, 45.3, 42.6, 19.8; **HRMS** (ESI pos) *m/z* calcd for $C_{28}H_{20}Br_2O$ $[M]^+$ 529.98754, found 529.98745.

9-(5-Methoxy-2-methyl-2,3-dihydro-1H-cyclopenta[a]naphthalen-1-ylidene)-9H-fluorene-3,6-dicarbonitrile (2_s)

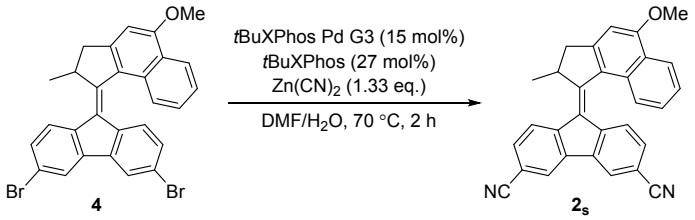

A N_2 filled Schlenk tube was charged with alkene **4** (42 mg, 79 µmol), *t*BuXPhos Pd G3 (9.4 mg, 12 µmol), *t*BuXPhos (9.0 mg, 21 µmol) and $Zn(CN)_2$ (12 mg, 0.10 mmol). A degassed (bubbling N_2 for 30 min) mixture of DMF/H_2O (99:1, 1.2 mL) was added and the resulting solution was heated to 70 °C for 2 h. After cooling to room temperature the mixture was diluted with EtOAc, washed with brine, dried over $MgSO_4$ and concentrated *in vacuo*. The crude product was purified by flash column chromatography (SiO_2, dry load on celite, 20–25% EtOAc in pentane) to obtain the final compound **2_s** (29 mg, 68 µmol, 86%) as a red-orange solid.

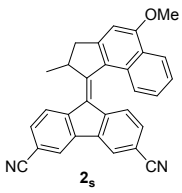

^{1}H NMR (600 MHz, $CDCl_3$) δ 8.40 (d, *J* = 8.4 Hz, 1H), 8.16 (d, *J* = 1.7 Hz, 1H), 8.08 (s, 1H), 8.08 (d, *J* = 8.4 Hz, 1H), 7.73 (dd, *J* = 8.2, 1.6 Hz, 1H), 7.51 (ddd, *J* = 8.3, 6.7, 1.2 Hz, 1H), 7.47 (d, *J* = 8.3 Hz, 1H), 7.37 (ddd, *J* = 8.3, 6.7, 1.3 Hz, 1H), 7.15 (dd, *J* = 8.3, 1.6 Hz, 1H), 7.01 (s, 1H), 6.75 (d, *J* = 8.3 Hz, 1H), 4.30 (p, *J* = 6.6 Hz, 1H), 4.15 (s, 3H), 3.62 (dd, *J* = 15.2, 5.4 Hz, 1H), 2.85 (d, *J* = 15.3 Hz, 1H), 1.46 (d, *J* = 6.7 Hz, 3H); **^{13}C NMR** (151 MHz, $CDCl_3$) δ 160.8, 160.1, 152.6, 143.4, 140.6, 137.8, 137.2, 131.3, 130.5, 130.2, 128.3, 127.4, 126.7, 125.9, 125.6, 125.0, 124.1, 123.8, 123.5, 123.2, 119.6, 109.4, 109.2, 102.8, 56.2, 45.6, 42.8, 20.2; **HRMS** (ESI pos) *m/z* calcd for $C_{30}H_{21}N_2O$ $[M+H]^+$ 425.16484, found 425.16539.

9-(5-Cyano-2-methyl-2,3-dihydro-1H-cyclopenta[a]naphthalen-1-ylidene)-9H-fluorene-3,6-dicarbonitrile (6_s)

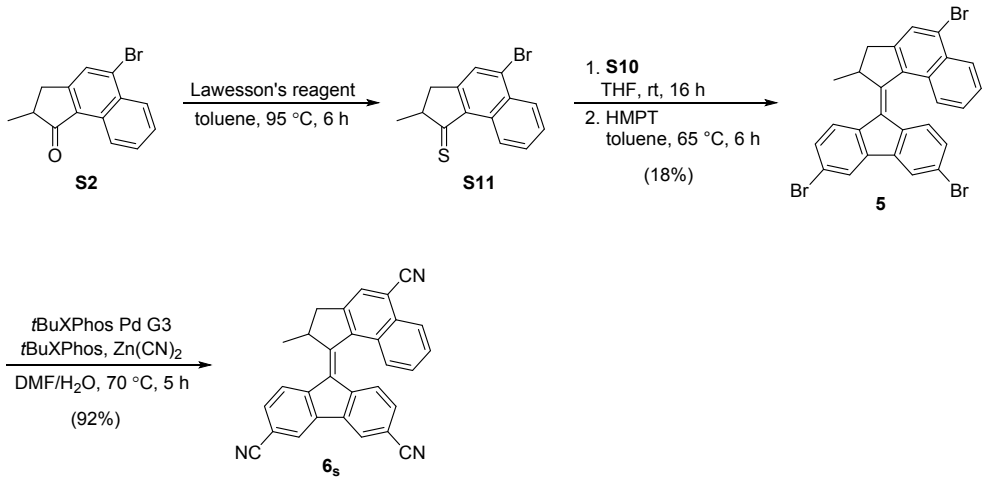

3,6-Dibromo-9-(5-bromo-2-methyl-2,3-dihydro-1H-cyclopenta[a]naphthalen-1-ylidene)-9H-fluorene (5)

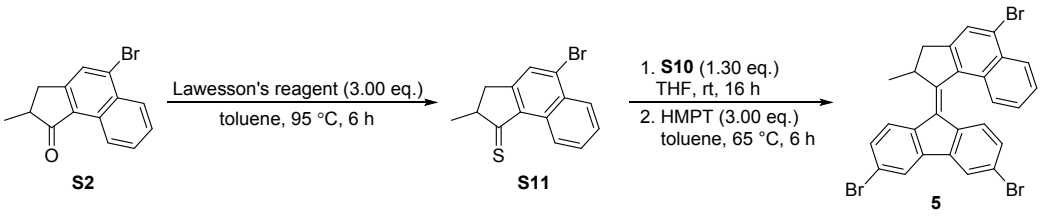

A mixture of ketone **S2** (120 mg, 0.436 mmol) and Lawesson's reagent (529 mg, 1.31 mmol) in anhydrous toluene (6.6 mL) was heated to 95 °C. After 6 h toluene was removed *in vacuo* and the thioketone intermediate **S11** was purified by flash column chromatography (SiO_2, dry load on celite, 2–10% DCM in pentane). It was then taken up in anhydrous THF (1.7 mL) and transferred to a Schlenk flask, followed by addition of diazo **S10** (198 mg, 0.567 mmol) dissolved in anhydrous THF (1.7 mL). The resulting mixture was stirred and room temperature for 16 h. Volatiles were removed *in vacuo*, the remaining solids were taken up in toluene (6.6 mL) and HMPT (238 µL, 1.31 mmol) was added. After stirring this mixture at 65 °C for 6 h volatiles were removed *in vacuo* and the desired product was purified by flash column chromatography (SiO_2, dry load on celite, 2–10% DCM in pentane). **5** (46 mg, 79 µmol, 18%) was obtained as a yellow solid. Data is in accordance with literature.[2]

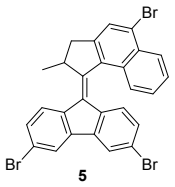

^{1}H NMR (600 MHz, $CDCl_3$) δ 8.37 (d, *J* = 8.5 Hz, 1H), 7.94 – 7.90 (m, 2H), 7.83 (d, *J* = 1.9 Hz, 1H), 7.80 (d, *J* = 8.3 Hz, 1H), 7.69 (d, *J* = 8.5 Hz, 1H), 7.62 – 7.56 (m, 1H), 7.53 (dd, *J* = 8.3, 2.0 Hz, 1H), 7.39 (ddd, *J* = 8.2, 6.7, 1.2 Hz, 1H), 6.92 (dd, *J* = 8.5, 1.9 Hz, 1H), 6.47 (d, *J* = 8.4 Hz, 1H), 4.25 (p, *J* = 6.5 Hz, 1H), 3.57 (dd, *J* = 15.1, 5.6 Hz, 1H), 2.76 (d, *J* = 15.2 Hz, 1H), 1.37 (d, *J* = 6.8 Hz, 3H); **^{13}C NMR** (151 MHz, $CDCl_3$) δ 151.8, 148.0, 140.8, 140.4, 138.6, 136.1, 135.9, 131.1, 130.6, 130.5, 129.5, 129.4, 128.5, 128.2, 127.9, 127.6, 127.2, 127.1, 126.3, 125.5, 123.3, 122.6, 121.4, 121.4, 45.6, 41.8, 19.3.

9-(5-Cyano-2-methyl-2,3-dihydro-1H-cyclopenta[a]naphthalen-1-ylidene)-9H-fluorene-3,6-dicarbonitrile (6_s)

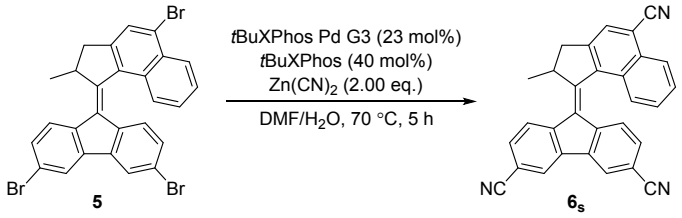

A N_2 filled Schlenk tube was charged with alkene **5** (30 mg, 52 µmol), *t*BuXPhos Pd G3 (9.4 mg, 12 µmol), *t*BuXPhos (8.8 mg, 21 µmol) and $Zn(CN)_2$ (12 mg, 0.10 mmol). A degassed (3x freeze-pump-thaw) mixture of DMF/H_2O (99:1, 780 µL) was added and the resulting solution was heated to 70 °C for 5 h. After cooling to room temperature the mixture was diluted with EtOAc (50 mL), washed with brine, dried over $MgSO_4$ and concentrated *in vacuo*. The crude product was purified by flash column chromatography (SiO_2, dry load on celite, 10–25% EtOAc in pentane containing 10% DCM) to obtain the final compound **6_s** (20 mg, 48 µmol, 92%) as an orange solid.

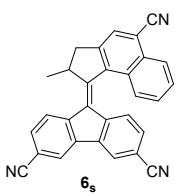

^{1}H NMR (600 MHz, $CDCl_3$) δ 8.41 (d, *J* = 8.4 Hz, 1H), 8.14 (d, *J* = 1.4 Hz, 1H), 8.08 (d, *J* = 8.1 Hz, 1H), 8.05 (d, *J* = 2.0 Hz, 2H), 7.77 (dd, *J* = 8.2, 1.5 Hz, 1H), 7.74 (ddd, *J* = 8.2, 6.9, 1.1 Hz, 1H), 7.69 (d, *J* = 8.4 Hz, 1H), 7.49 (ddd, *J* = 8.2, 6.9, 1.1 Hz, 1H), 7.14 (dd, *J* = 8.2, 1.5 Hz, 1H), 6.66 (d, *J* = 8.2 Hz, 1H), 4.37 (p, *J* = 6.6 Hz, 1H), 3.67 (dd, *J* = 15.4, 5.5 Hz, 1H), 2.92 (d, *J* = 15.4 Hz, 1H), 1.44 (d, *J* = 6.8 Hz, 3H); **^{13}C NMR** (151 MHz, $CDCl_3$) δ 156.6, 147.3, 142.9, 140.3, 140.1, 139.0, 138.5, 132.0, 132.0, 131.0, 130.8, 130.2,

129.3, 129.1, 128.7, 127.4, 126.7, 126.3, 124.9, 124.0, 123.5, 119.0, 118.9, 117.7, 113.6, 111.4, 111.3, 46.1, 41.9, 19.3; **HRMS** (ESI pos) *m/z* calcd for $C_{30}H_{17}N_3Na$ $[M+H]^+$ 442.13147, found 442.13172.

3. DFT Calculations

3.1. Methods

Structure optimizations of stable and metastable isomers were performed in Gaussian 16 (B3LYP, 6-311G++(d,p)) using the GaussView 5.0 add-on.[8,9] Transition states (TS) were localized by scanning the dihedral angle around the overcrowded alkene and structures were optimized to transition state (TS) (Berny, B3LYP, 6-311G++(d,p)). UV-vis and CD spectra of the optimized structures were obtained by time dependent DFT calculations (CAM-B3LYP, 6-311G++(d,p)) using the Polarizable Continuum Model (PCM) employing the integral equation formalism variant (IEFPCM) to model DCM as solvent.

3.2. Comparison of Calculated Energies

Figure S1 shows the calculated energy profiles for THI of motors **1**, **2**, and **6**. Table S1 contains the sums of electronic and thermal free energies ($\varepsilon_0 + G_{corr}$) for metastable and stable isomers as well as thermal helix inversion (THI) TS structures of motors **1**, **2** and **6**.

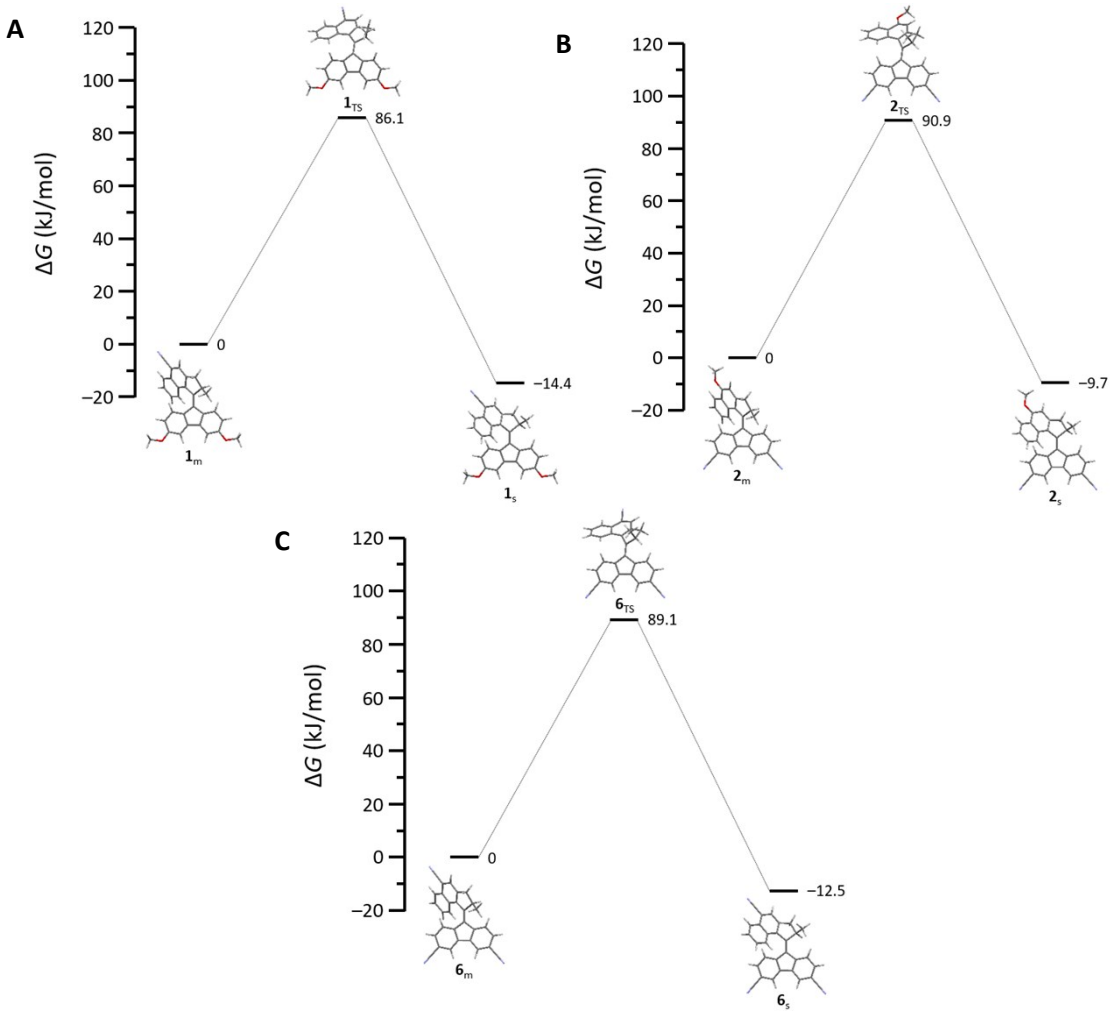

Figure S1. Calculated energy profiles for THI of motors **1** (**A**), **2** (**B**) and **6** (**C**).

Table S1. Sums of electronic and thermal free energies (ε_0 + G_{corr}) for metastable and stable isomers as well as THI TS structures of motors **1**, **2** and **6** in Hartrees.

	1	**2**	**6**
metastable	-1362.173157	-1339.921249	-1317.658406
TS	-1362.140353	-1339.886608	-1317.624482
stable	-1362.178623	-1339.924945	-1317.663159

3.3. Comparison of Calculated Structures

Figure S2 shows overlays of $\mathbf{1_s}$, $\mathbf{2_s}$ and $\mathbf{6_s}$ generated using Pymol (v.099rc6).[10]

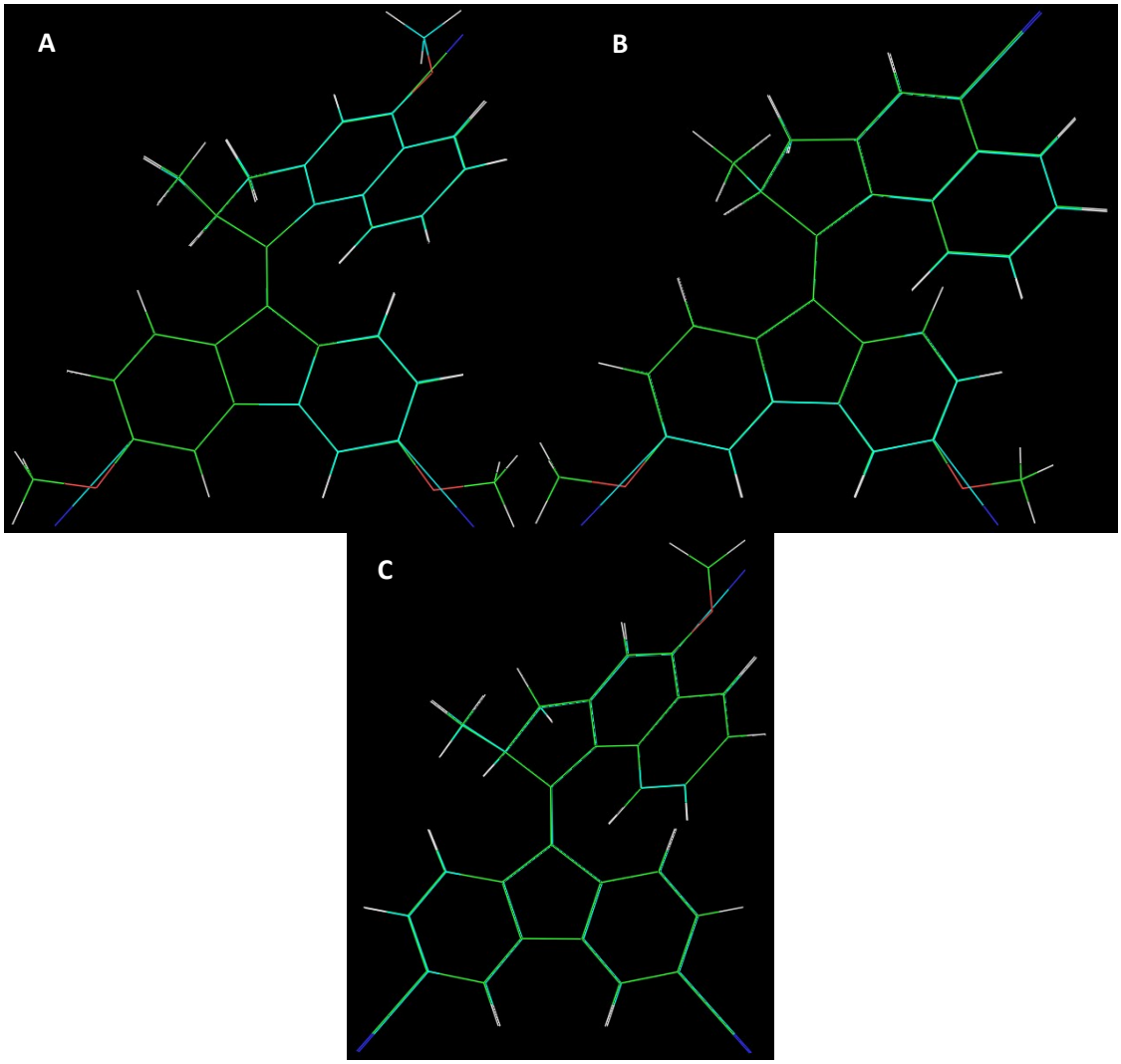

Figure S2. Comparison of DFT structures of $\mathbf{1_s}$ and $\mathbf{2_s}$ (**A**), $\mathbf{1_s}$ and $\mathbf{6_s}$ (**B**) as well as $\mathbf{2_s}$ and $\mathbf{6_s}$ (**C**).

Table S2 contains the root-mean-square deviations between the motor core structures of $\mathbf{1_s}$, $\mathbf{2_s}$ and $\mathbf{6_s}$ as calculated using GROMACS.[11,12]. These core structures were obtained by replacing OMe and CN substituents with H following structural optimization as described in *Section 3.1.*.

Table S2. Root-mean-square deviations between core structures of $\mathbf{1}_s$, $\mathbf{2}_s$ and $\mathbf{6}_s$.

	$\mathbf{2}_s$	$\mathbf{6}_s$
$\mathbf{1}_s$	0.00195	0.00159
$\mathbf{2}_s$		0.00178

Figure S3 and S4 show overlays of $\mathbf{1}_{TS}$, $\mathbf{2}_{TS}$ and $\mathbf{6}_{TS}$ generated using Pymol (v.099rc6).[10]

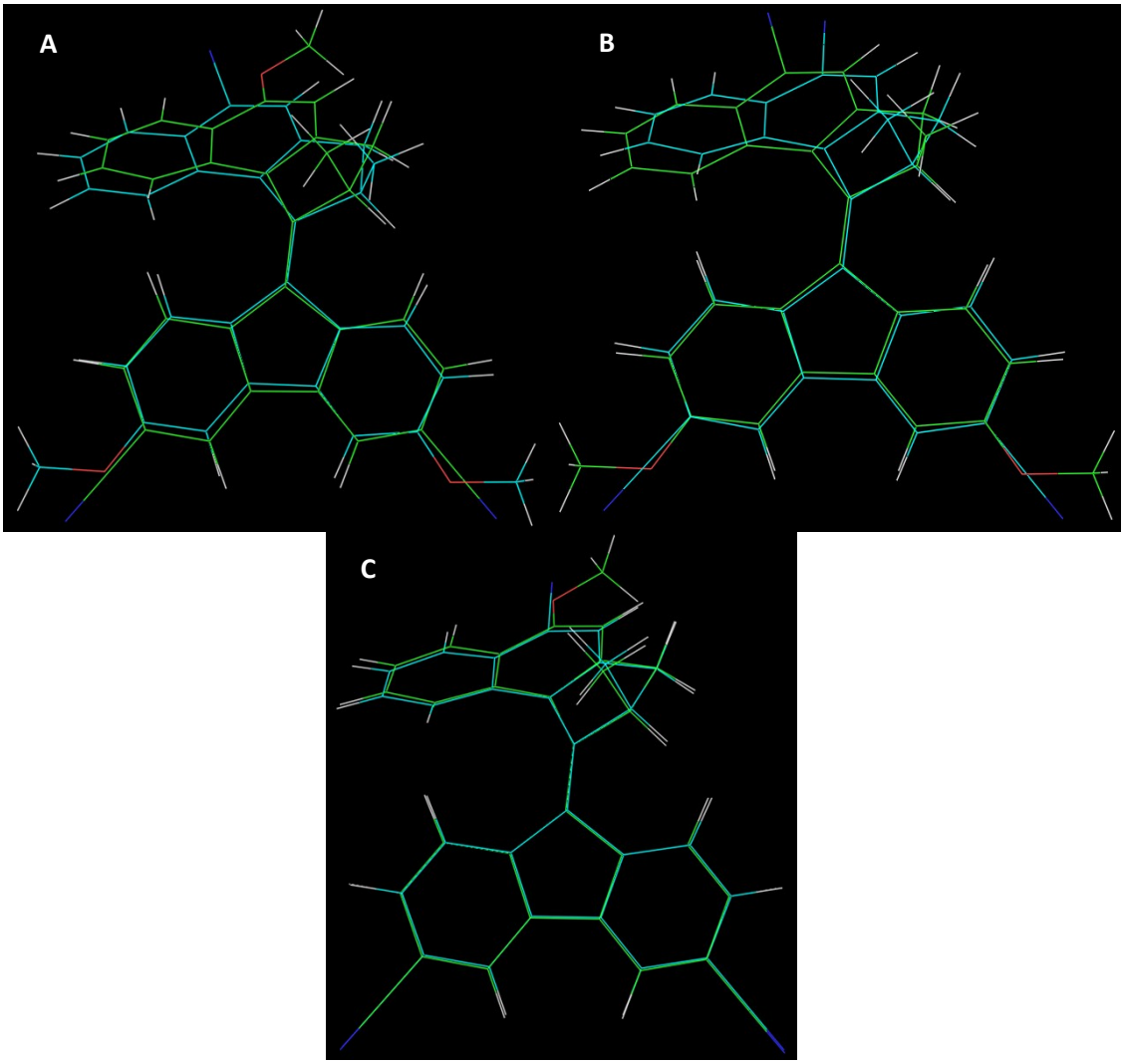

Figure S3. Comparison of DFT structures (front view) of $\mathbf{1}_{TS}$ and $\mathbf{2}_{TS}$ (**A**), $\mathbf{1}_{TS}$ and $\mathbf{6}_{TS}$ (**B**) as well as $\mathbf{2}_{TS}$ and $\mathbf{6}_{TS}$ (**C**).

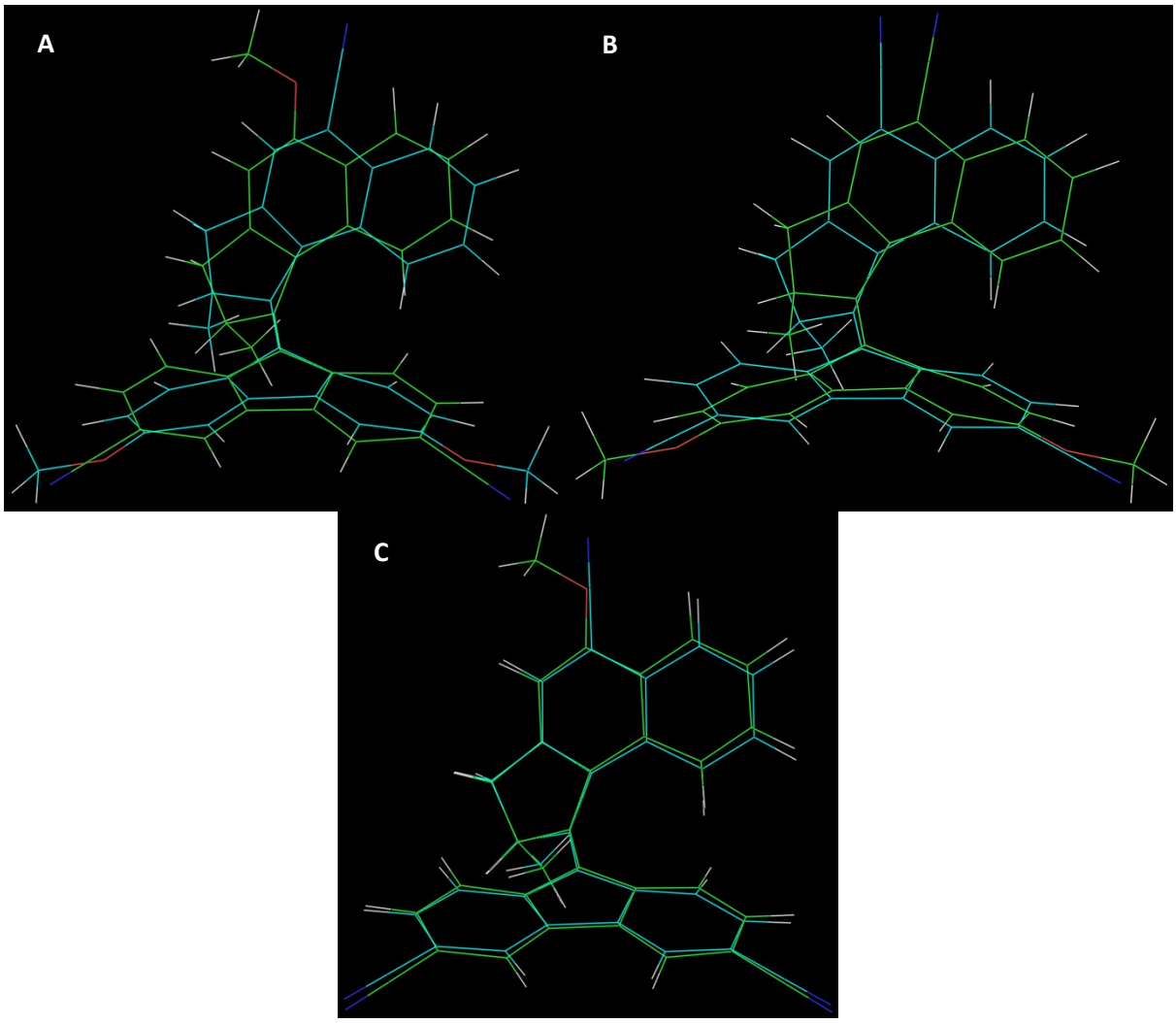

Figure S4. Comparison of DFT structures (rear view) of $\mathbf{1}_{TS}$ and $\mathbf{2}_{TS}$ (**A**), $\mathbf{1}_{TS}$ and $\mathbf{6}_{TS}$ (**B**) as well as $\mathbf{2}_{TS}$ and $\mathbf{6}_{TS}$ (**C**).

Table S3 contains the root-mean-square deviations between the motor core structures of $\mathbf{1}_{TS}$, $\mathbf{2}_{TS}$ and $\mathbf{6}_{TS}$ as calculated using GROMACS.[11,12]. These core structures were obtained by replacing OMe and CN substituents with H following structural optimization as described in *Section 3.1.*.

Table S3. Root-mean-square deviations between core structure of $\mathbf{1}_{TS}$, $\mathbf{2}_{TS}$ and $\mathbf{6}_{TS}$.

	$\mathbf{2}_{TS}$	$\mathbf{6}_{TS}$
$\mathbf{1}_{TS}$	0.23913	0.17497
$\mathbf{2}_{TS}$		0.01062

Figure S5 shows overlays of $\mathbf{1}_{m}$, $\mathbf{2}_{m}$ and $\mathbf{6}_{m}$ generated using Pymol (v.099rc6).[10]

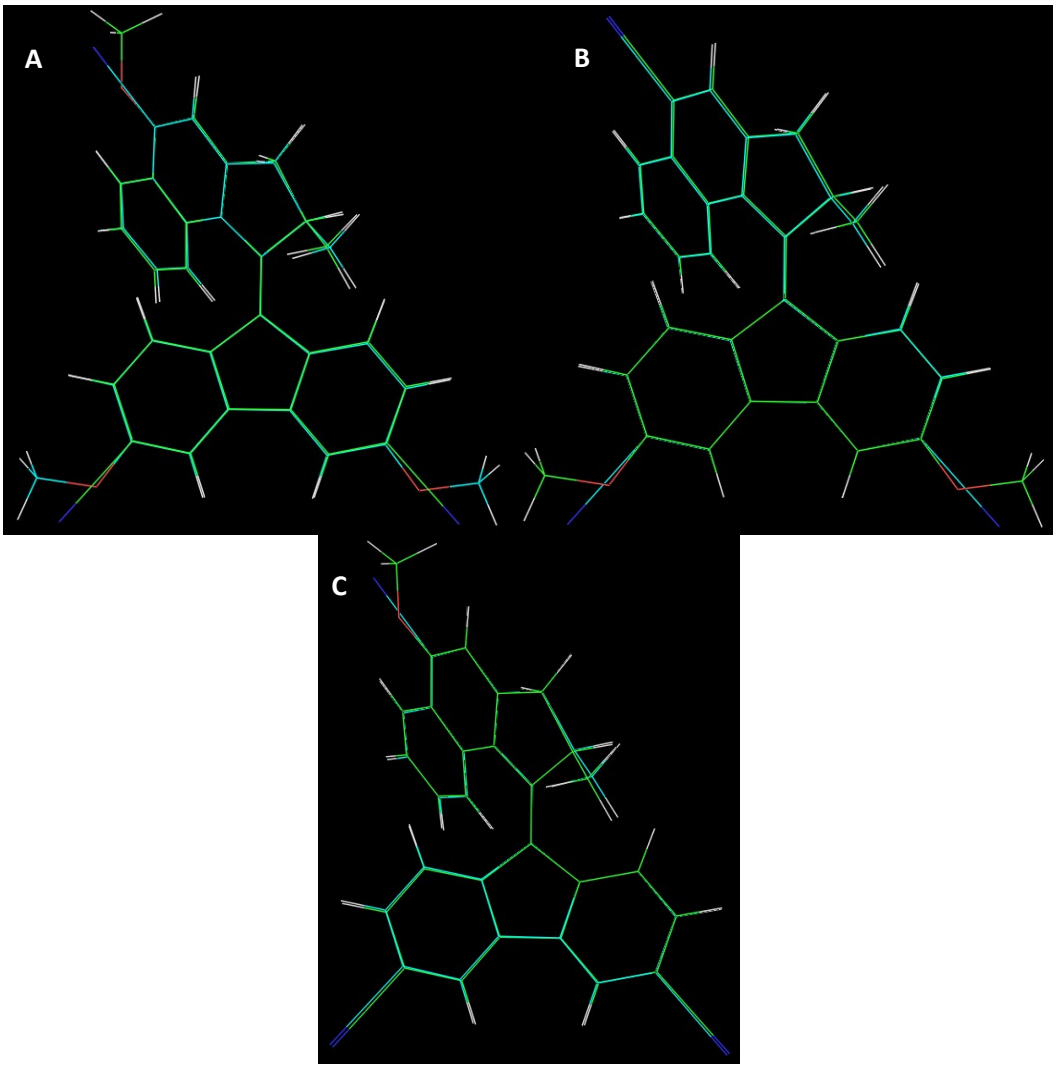

Figure S5. Comparison of DFT structures of $\mathbf{1}_m$ and $\mathbf{2}_m$ (**A**), $\mathbf{1}_m$ and $\mathbf{6}_m$ (**B**) as well as $\mathbf{2}_m$ and $\mathbf{6}_m$ (**C**).

Table S4 contains the root-mean-square deviations between the motor core structures of $\mathbf{1}_m$, $\mathbf{2}_m$ and $\mathbf{6}_m$ as calculated using GROMACS.[11,12] These core structures were obtained by replacing OMe and CN substituents with H following structural optimization as described in *Section 3.1.*.

Table S4. Root-mean-square deviations between core structures of $\mathbf{1}_m$, $\mathbf{2}_m$ and $\mathbf{6}_m$.

	$\mathbf{2}_m$	$\mathbf{6}_m$
$\mathbf{1}_m$	0.00424	0.00167
$\mathbf{2}_m$		0.00335

Bond lengths of the central C–C bond connecting the two motor halves in DFT optimized structures of stable and metastable isomers as well as the TS of THI of motors **1**, **2** and **6** are summarized in Table S5.

Table S5. Summary of central C–C bond lengths in DFT optimized structures of stable and metastable isomers as well as the TS of THI of motors **1**, **2** and **6**.

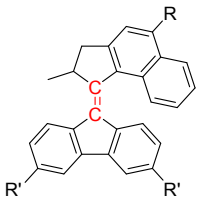

1: R = CN, R' = OMe
2: R = OMe, R' = CN
6: R = R' = CN

	$(C=C)_S$ [Å]	$(C=C)_{TS}$ [Å]	$(C=C)_m$ [Å]
1	1.3669	1.3820	1.3751
2	1.3734	1.3936	1.3833
6	1.3690	1.3867	1.3778

The sums of Mulliken charges of stator and rotor halves of metastable and stable isomers as well as THI TS structures of motors **1**, **2** and **6** are summarized in Table S6.

Table S6. Sums of Mulliken charges of stator and rotor halves of metastable and stable isomers as well as THI TS structures of motors **1**, **2** and **6**.

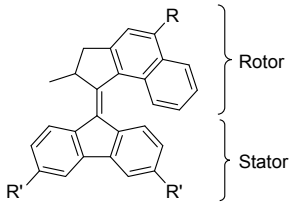

1: R = CN, R' = OMe
2: R = OMe, R' = CN
6: R = R' = CN

	1		**2**		**6**	
	stator	*rotor*	*stator*	*rotor*	*stator*	*rotor*
metastable	0.101211	-0.10121	-0.332878	0.332876	0.030369	-0.030371
TS	0.266162	-0.266163	-0.670095	0.670092	-0.637904	0.637905
stable	0.143654	-0.143653	-0.361828	0.36183	-0.189678	0.189679

4. UV-vis Studies

4.1. Initial Studies

A $1.0 \cdot 10^{-5}$ M solution of the according molecular motor in DCM was prepared. UV-vis spectra were recorded at 20 °C before and during irradiation with 420 nm ($\mathbf{1}_s$, $\mathbf{6}_s$) and 455 nm LED ($\mathbf{2}_s$), respectively. The obtained stacks of spectra are shown in Figure S6.

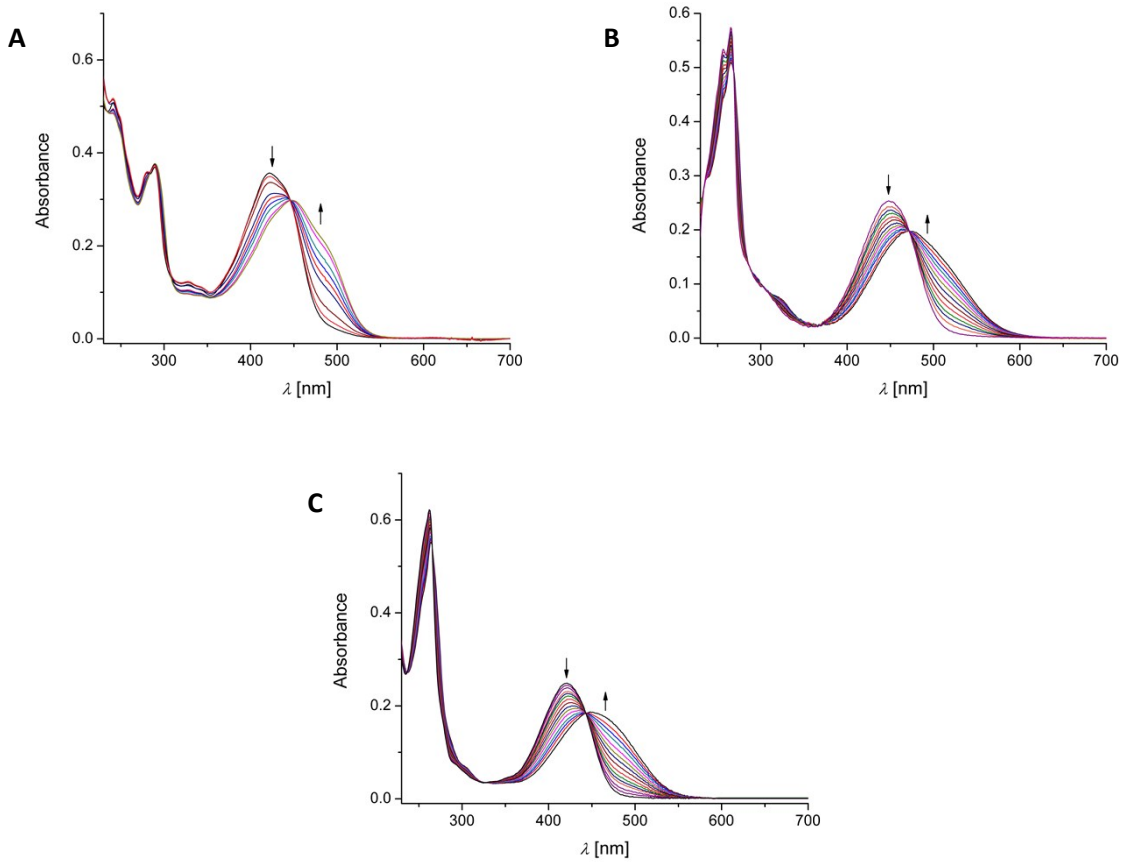

Figure S6. Stacks of UV-vis spectra (DCM, c = $1.0 \cdot 10^{-5}$ M) showing switching from $\mathbf{1_s}$ (**A**), $\mathbf{2_s}$ (**B**) and $\mathbf{6_s}$ (**C**) to their respective metastable isomers when irradiated at 20 °C with 420 nm ($\mathbf{1_s}$ and $\mathbf{6_s}$) or 455 nm LED ($\mathbf{2_s}$), respectively.

4.2. Eyring Plots

A $1.0 \cdot 10^{-5}$ M solution of the according molecular motor in DCM was prepared. Samples of each molecular motor at five different temperatures were at first irradiated to PSS (420 nm LED ($\mathbf{1_s}$, $\mathbf{6_s}$) or 455 nm LED ($\mathbf{2_s}$)) and the subsequent thermal helix inversion back to the stable isomer was followed on a UV-vis spectrophotometer. Rate constants, *k*, as changes of absorbance over time were determined by fitting a 1st order rate law and plotted to determine the thermodynamic parameters of the thermal helix inversion. Errors were determined using the Monte Carlo method. Eyring plots are shown in Figure S7.

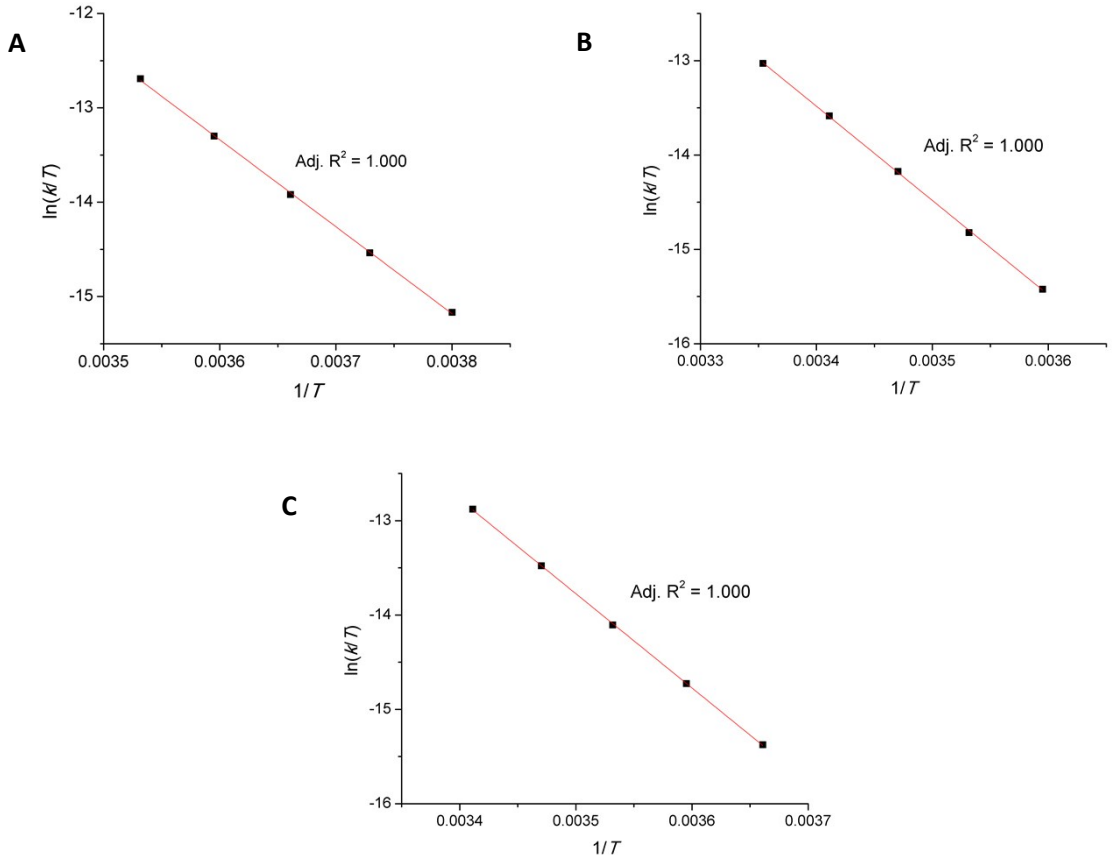

Figure S7. Eyring plots for thermal helix inversion of $\mathbf{1_m}$ (**A**), $\mathbf{2_m}$ (**B**) and $\mathbf{6_m}$ (**C**) measured on UV-vis spectrophotometer (DCM, c = $1.0 \cdot 10^{-5}$ M, 420 nm LED ($\mathbf{1_s}$, $\mathbf{6_s}$) or 455 nm LED ($\mathbf{2_s}$)).

4.3. Quantum Yields

Ferrioxalate Actinometer[13]

A 10 mm quartz cuvette containing 2.00 mL of a 20 mM (420 nm LED) or 40 mM (455 nm LED) solution of $K_3[Fe(C_2O_4)_3] \cdot 3H_2O$ in 50 mM aq. H_2SO_4 was placed in the sample holder of a UV-vis spectrophotometer and left to equilibrate at 20 °C (900 rpm stirring). The sample was irradiated with an LED of the according wavelength for a given amount of time, before 10 µL were added to 2.00 mL of a solution of 1,10-phenanthroline (phen, 1.00 g/L) and NaOAc (122.5 g/L) in 0.50 M aq. H_2SO_4 in an additional quartz cuvette. The same was done with 10 µL of the non-irradiated stock solution and both samples were kept in the dark for 15 min. They were then placed in the sample holder of the UV-vis spectrophotometer, equilibrated to 20 °C and their absorption spectra were measured. Plots of the absorbance of the irradiated sample at 517 nm after subtracting the blank (ΔA_{517nm}) as a function of irradiation time (t) can be found in Figure S8.

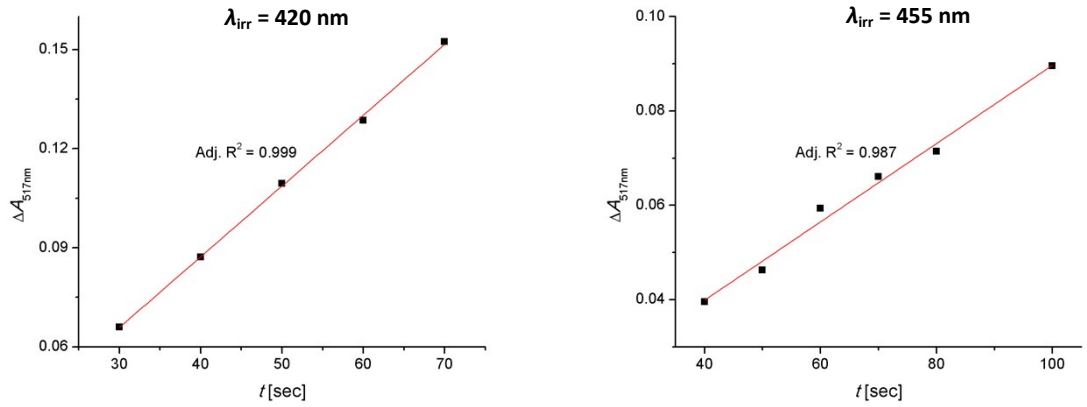

Figure S8. Increasing absorbance at 517 nm associated with formation of $[Fe(phen)_3]^{2+}$ due to formation of free Fe^{2+} upon irradiation of $K_3[Fe(C_2O_4)_3]\cdot 3H_2O$ with 420 nm (20 mM) and 455 nm LED (40 mM), respectively.

For each data point one can now calculate the concentration of Fe^{2+} ions, $c(Fe^{2+})$, using l = 1.0 cm and $\varepsilon(517nm)$=11100 $L\cdot mol^{-1}\cdot cm^{-1}$ according to Eq. 1.[13]

$$c(Fe^{2+}) = \frac{\Delta A(517nm)}{l * \varepsilon(517nm)} \qquad \text{Eq. 1}$$

From this the amount of Fe^{2+} ions, $n(Fe^{2+})$, can be calculated according to Eq. 2 where V_1 is the irradiated volume, V_2 is the volume taken for determination of ferric ions from the irradiated sample and V_3 is the final volume after complexation with phenanthroline.

$$n(Fe^{2+}) = \frac{c(Fe^{2+}) * V_3 * V_1}{V_2} \qquad \text{Eq. 2}$$

From this the photon flux, $N(h\nu)/t$, can be calculated according to Eq. 3 with the quantum yield of $K_3[Fe(C_2O_4)_3]$, φ, equaling 1.12 and t being the irradiation time of the according time point.[13]

$$\frac{N(h\nu)}{t} = \frac{n(Fe^{2+})}{\varphi * t} \qquad \text{Eq. 3}$$

The averaged photon flux for irradiation at 420 nm and 455 nm, respectively, is given in Table S7.

Table S7. Summary of averaged photon fluxes for irradiation experiments at 420 nm and 455 nm.

	420 nm	**455 nm**
$N(h\nu)/t$ [$mol\cdot s^{-1}$]	$(7.007 \pm 0.061)\cdot 10^{-8}$	$(3.106 \pm 0.129)\cdot 10^{-8}$

Motors

A 10 mm quartz cuvette containing 2.00 mL of a $2.0\cdot 10^{-4}$ M solution of the corresponding motor in DCM was placed in the sample holder of a UV-vis spectrophotometer and left to equilibrate at 20 °C (900 rpm stirring). The sample was then irradiated with an appropriate LED (**1**$_s$, **6**$_s$: 420 nm; **2**$_s$: 455 nm) under the exact some conditions that the according reference sample had been irradiated. A UV-vis spectrum was measured every 2.5 s for 5 min and the initial linear absorbance increase was plotted as a function of irradiation time (Figure S9).

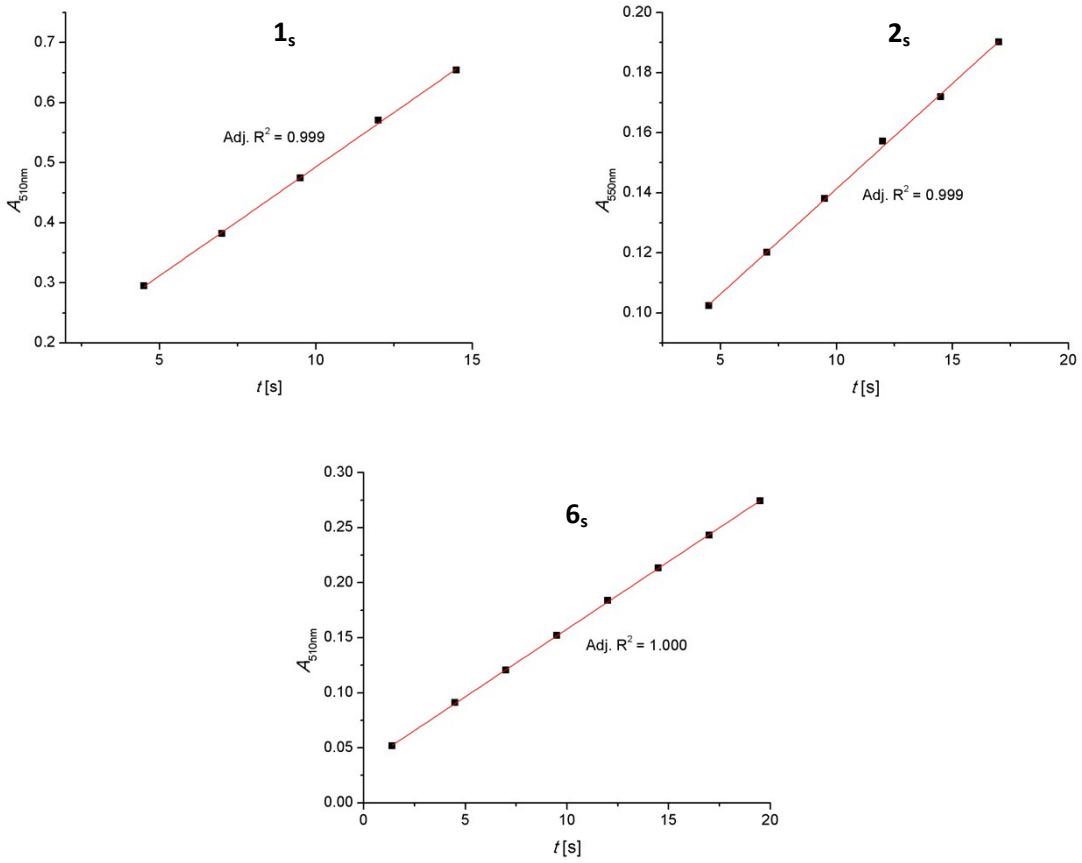

Figure S9. Linear increase of absorbance at 510 nm (**1**$_s$, **6**$_s$) and 550 nm (**2**$_s$) corresponding to the formation of **1**$_m$, **2**$_m$, and **6**$_m$ in the early stages of irradiation with a 420 nm (**1**$_s$, **6**$_s$) and 455 nm LED (**2**$_s$), respectively.

Molar absorption coefficients of stable (ε_s) and metastable (ε_m) motor isomers were determined by measuring UV-vis spectra of $1.0 \cdot 10^{-5}$ M solutions of these motors in DCM before and after irradiation (**1**$_s$, **6**$_s$: 420 nm; **2**$_s$: 455 nm) to PSS at –10 °C (Table S8). For ratios of metastable:stable isomers at PSS see Section 5.

Table S8. Molar absorption coefficient of stable and metastable isomers of motors **1**, **2** and **6** at indicated wavelengths.

	ε_s [mol^{-1}·cm^{-1}]	ε_m [mol^{-1}·cm^{-1}]
1	248 ± 60 (510 nm), 21058 ± 25 (420 nm)	9263 ± 64 (510 nm), 10249 ± 46 (420 nm)
2	181 ± 61 (550 nm), 22266 ± 37 (455 nm)	7964 ± 55 (550 nm), 13117 ± 59 (455 nm)
6	178 ± 57 (510 nm), 18760 ± 33 (420 nm)	7354 ± 32 (510 nm), 8503 ± 28 (420 nm)

Eq. 4 allows conversion of the increase of absorbance into an increase of the fraction of formed metastable isomer, η_m. A and ε are the absorbance and molar absorption coefficients of stable (ε_s) and metastable (ε_m) isomers at the according wavelength, respectively. c is the total concentration of molecular motor in the sample.

$$\eta_m = \frac{A - \varepsilon_s * c}{\epsilon_m * c - \varepsilon_s * c}$$ Eq. 4

Using the volume (V) and the total concentration (c) of the sample this can then be converted into the amount of formed metastable isomer (n_m) according to Eq. 5 (Figure S10).

$$n_m = \eta_m * c * V$$ Eq. 5

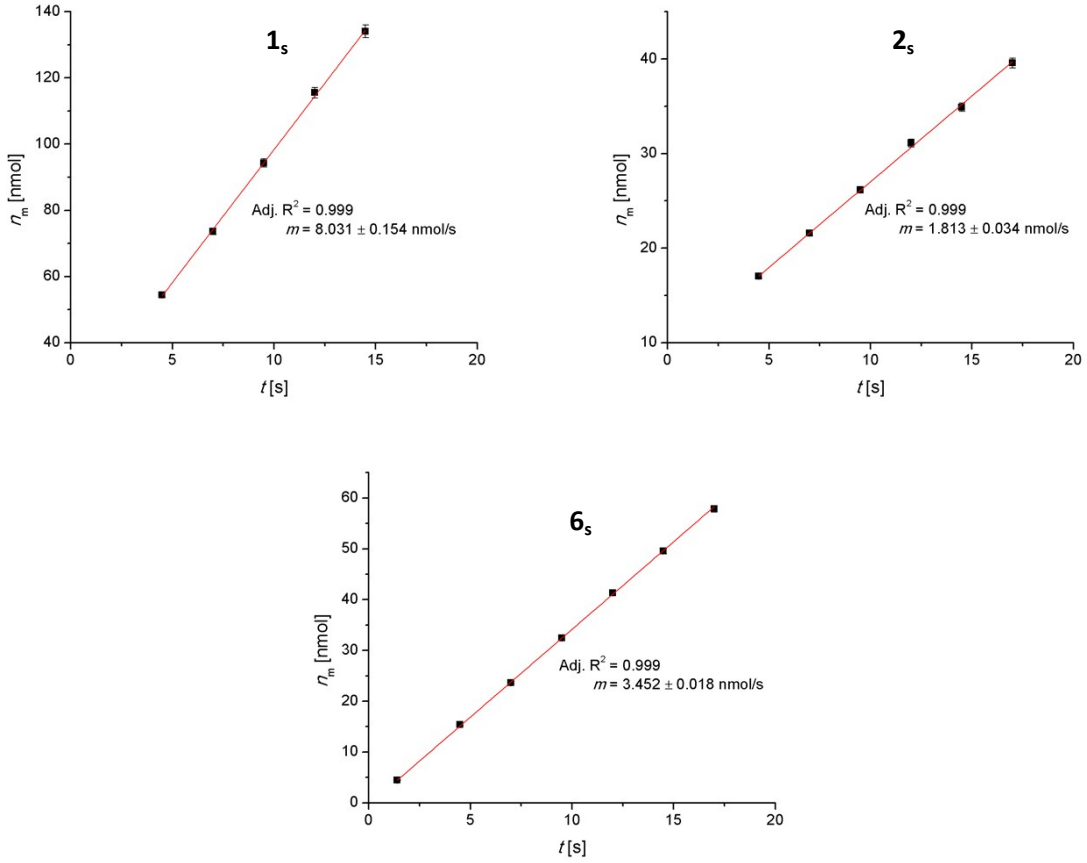

Figure S10. Linear increase of amount of **1**$_m$, **2**$_m$ and **6**$_m$ in the early stages of irradiation of samples of **1**$_s$, **2**$_s$ and **6**$_s$ with 420 nm (**1**$_s$, **6**$_s$) and 455 nm LED (**2**$_s$), respectively.

The slope, m, of the fitted lines in Figure S10 can be used to calculate the quantum yield for the formation of the metastable isomer, $\varphi_{s\rightarrow m}$, according to Eq. 6 using the appropriate photon flux from Table S7.

$$\varphi_{s\rightarrow m} = \frac{m}{N(h\nu)/t}$$ Eq. 6

The quantum yield for the back-reaction, $\varphi_{m\rightarrow s}$, can be obtained according to Eq. 7 using the molar absorption coefficients of the stable (ε_s) and metastable (ε_m) isomers at the wavelength used for irradiation (Table S8) as well as the fractions of stable and metastable isomers of the PSS mixture, $\eta_{PSS,s}$ and $\eta_{PSS,m}$, respectively.

$$\varphi_{m\to s} = \varphi_{s\to m} * \frac{\eta_{PSS,s} * \varepsilon_s}{\eta_{PSS,m} * \varepsilon_m} \qquad \text{Eq. 7}$$

4.4. Fatigue Studies

A 10 mm quartz cuvette containing a $1.0\cdot10^{-5}$ M solution of the according motor in DCM was placed in the sample holder of a UV-vis spectrophotometer and the solution was warmed up to the indicated temperature (**1**$_s$: 25 °C; **2**$_s$: 35 °C; **6**$_s$: 30 °C). After equilibration a spectrum was measured and the sample subsequently irradiated to PSS (5 min) using an appropriate LED (**1**$_s$, **6**$_s$: 420 nm; **2**$_s$: 455 nm). Another spectrum was measured, the light source was removed and the sample kept at the above temperature. After full isomerization back to the stable isomer had occurred another spectrum was collected and this sequence was repeated a total of ten times, corresponding to ten 180° rotations. Figure S11 shows the changes in absorbance at 420 nm (**1**$_s$, **6**$_s$) and 450 nm (**2**$_s$), respectively, over these ten cycles.

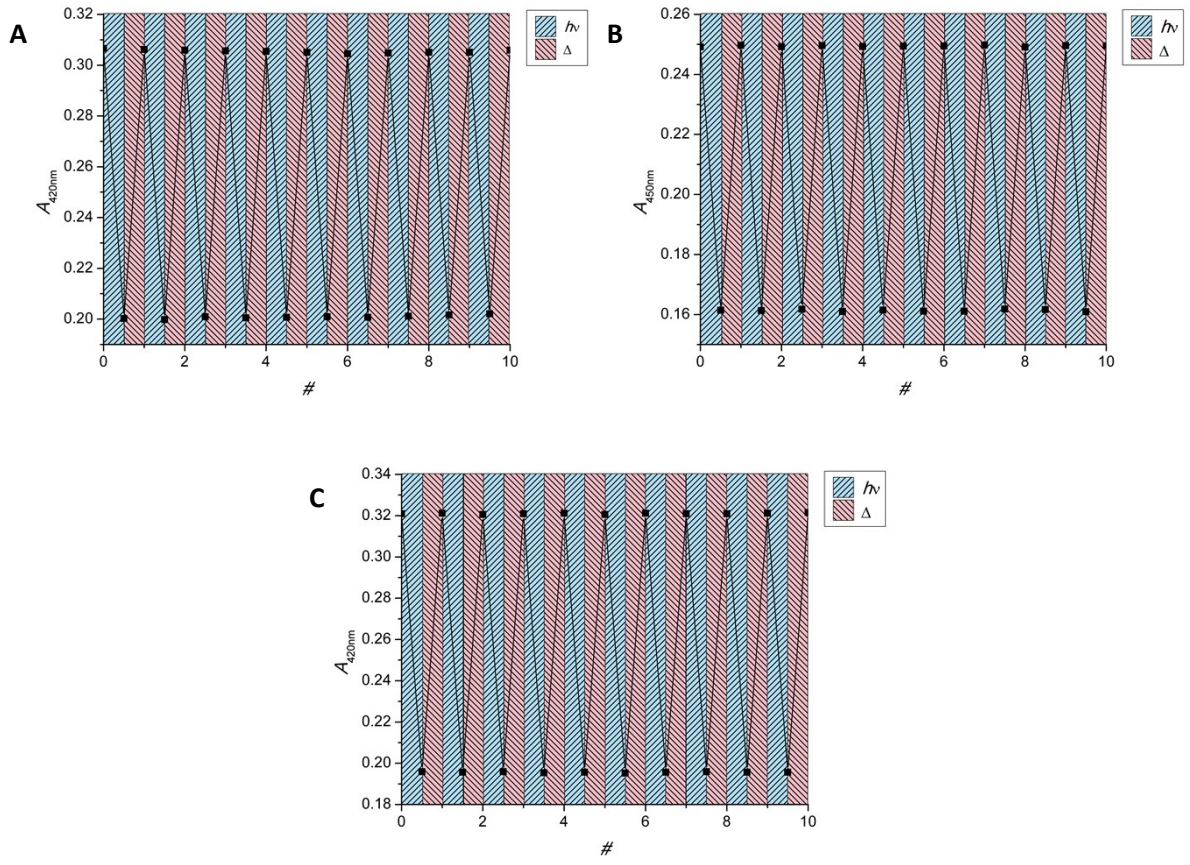

Figure S11. A, **C:** Fatigue studies on **1**$_s$ (**A**) and **6**$_s$ (**C**). Conditions: DCM, 25 °C (**1**$_s$), 30 °C (**6**$_s$), $1.0\cdot10^{-5}$ M, 420 nm LED (0.35 A, 5 min irr.). **B**: Fatigue study on **2**$_s$. Conditions: DCM, 35 °C, $1.0\cdot10^{-5}$ M, 455 nm LED (0.35 A, 5 min irr.).

5. NMR Studies

A $1.0 \cdot 10^{-3}$ M solution of the corresponding motor in DCM-d_2 was prepared and transferred into an NMR tube which was subsequently fitted with a glass fibre cable for *in situ* irradiation. The sample was placed in a Varian Unity Plus 500 NMR spectrometer and cooled to –10 °C. ^{1}H NMR spectra were recorded before irradiation and after irradiation to PSS using an appropriate LED (**1**$_s$, **6**$_s$: 420 nm; **2**$_s$: 455 nm). An irradiation time of 90 min was used to ensure PSS would be reached at the comparably high concentration of these samples. This time was not optimized. The sample was then warmed to room temperature for 75 min to allow for complete THI before recording another ^{1}H NMR spectrum at –10 °C.

Note: At this point it is important to distinguish between the photochemical back-reaction from the metastable isomer to the stable isomer which does not lead to unidirectional rotation of the motor but rather a back and forth type switching and the thermal helix inversion leading to unidirectional rotation (see Scheme 1). A photochemical back-reaction could indeed be performed very well with motor **6** (as well as **1** and **2**) as the UV-vis spectra of stable and metastable isomers show a significant band separation. This is highlighted by the metastable isomer being dominant at PSS when irradiating with 420 nm with the outcome being reversed at 490 nm, where the metastable isomer has a significantly higher molar absorption coefficient. Indeed, irradiating at a slightly higher wavelength than 490 nm should lead to a complete back-reaction to the stable isomer. To achieve unidirectional rotation the initial photochemical step has to be followed by a thermal step (thermal helix inversion), which for the present three motors leads to a compound indistinguishable from the original stable isomer. The following photochemical step which initiates the second 180° rotation can therefore be performed using light of the same wavelength as for the first step. A strongly favoured photochemical forward reaction can therefore be considered highly beneficial for the overall performance of an overcrowded alkene based molecular motor of this type.

Figures S12–S14 show representative spectra stacks for irradiation near the respective absorption maximum of motors **1**$_s$, **2**$_s$ and **6**$_s$. Spectra before irradiation and after completed THI did not contain detectable amounts of metastable isomers.

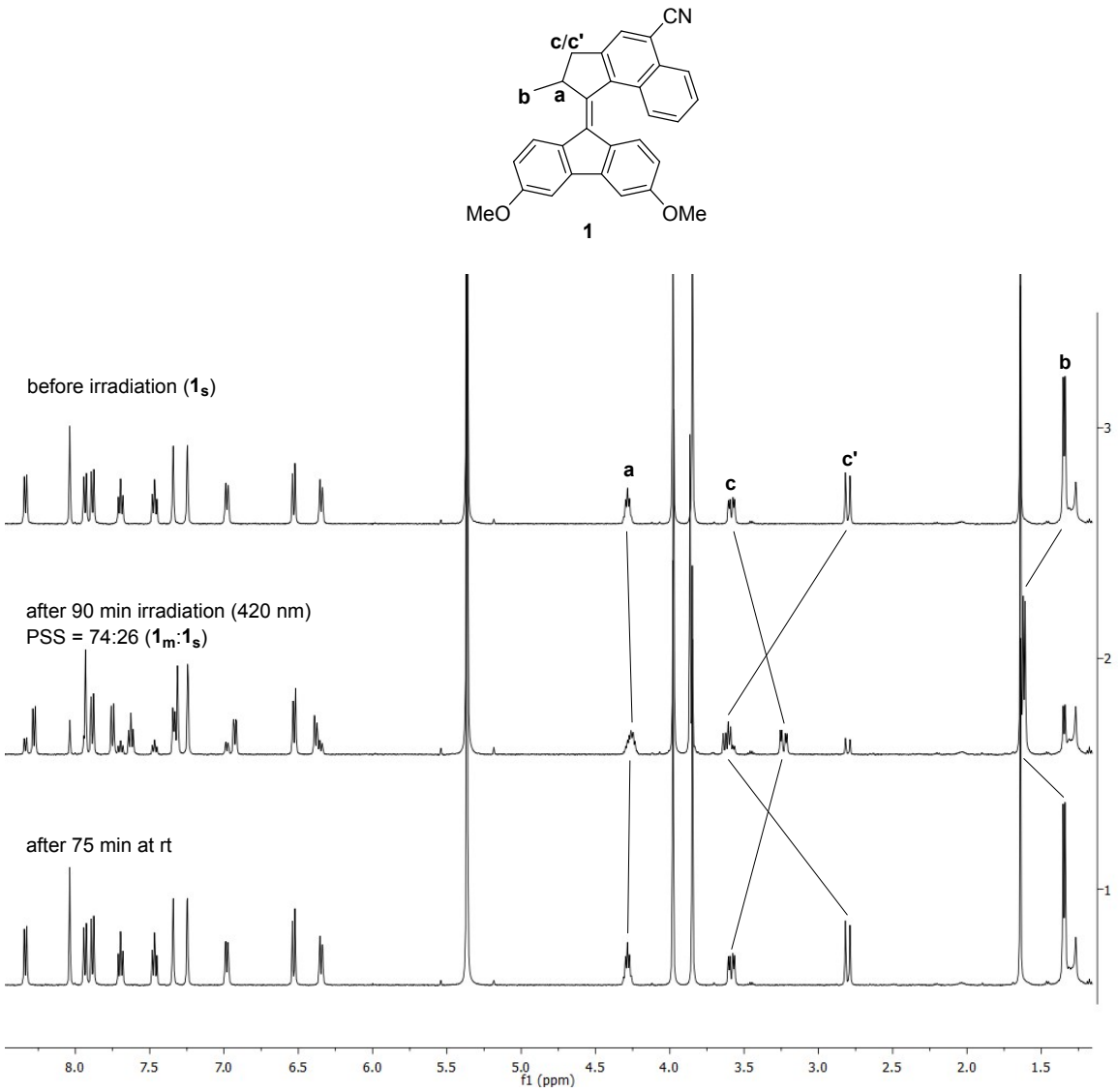

Figure S12. Stack of ^{1}H NMR spectra of **1** recorded at –10 °C before irradiation (**1**$_s$), at PSS and after completed THI.

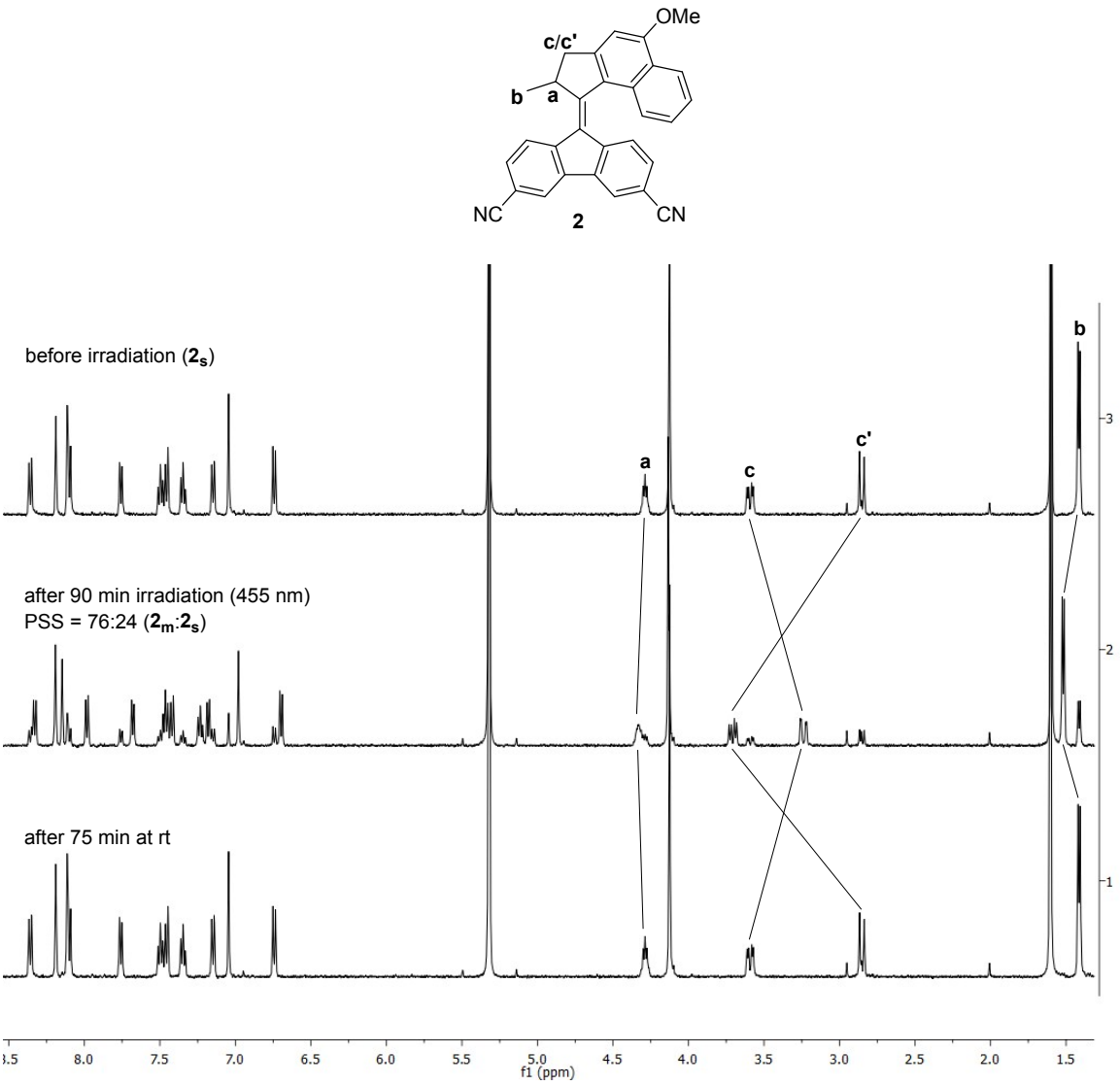

Figure S13. Stack of ^{1}H NMR spectra of **2** recorded at –10 °C before irradiation ($\mathbf{2_s}$), at PSS and after completed THI.

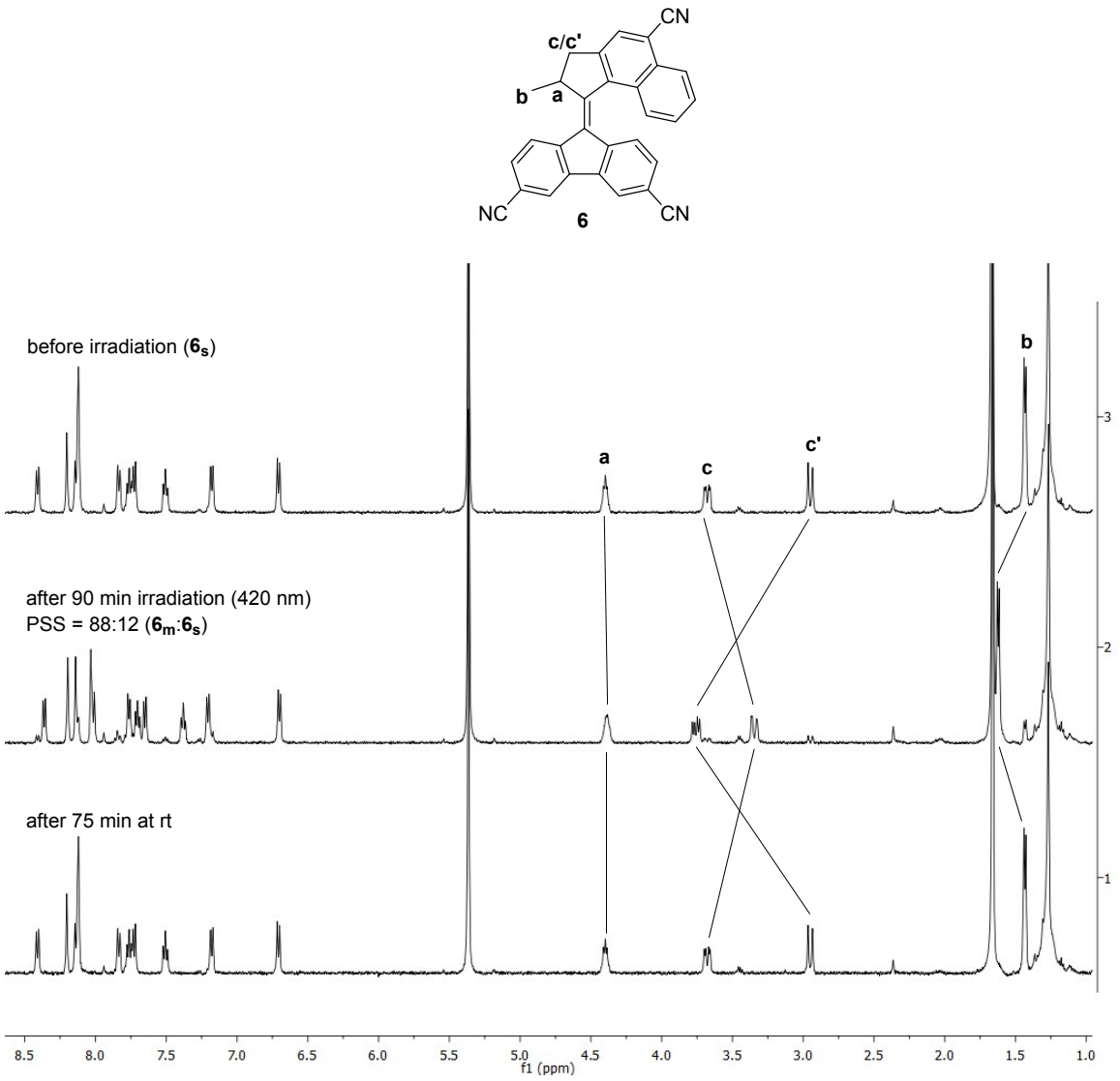

Figure S14. Stack of ^{1}H NMR spectra of **6** recorded at –10 °C before irradiation (**6**$_s$), at PSS and after completed THI.

Figure 15 shows spectra of a sample of **2**$_s$ recorded before irradiation, at PSS (530 nm LED) and after completed THI.

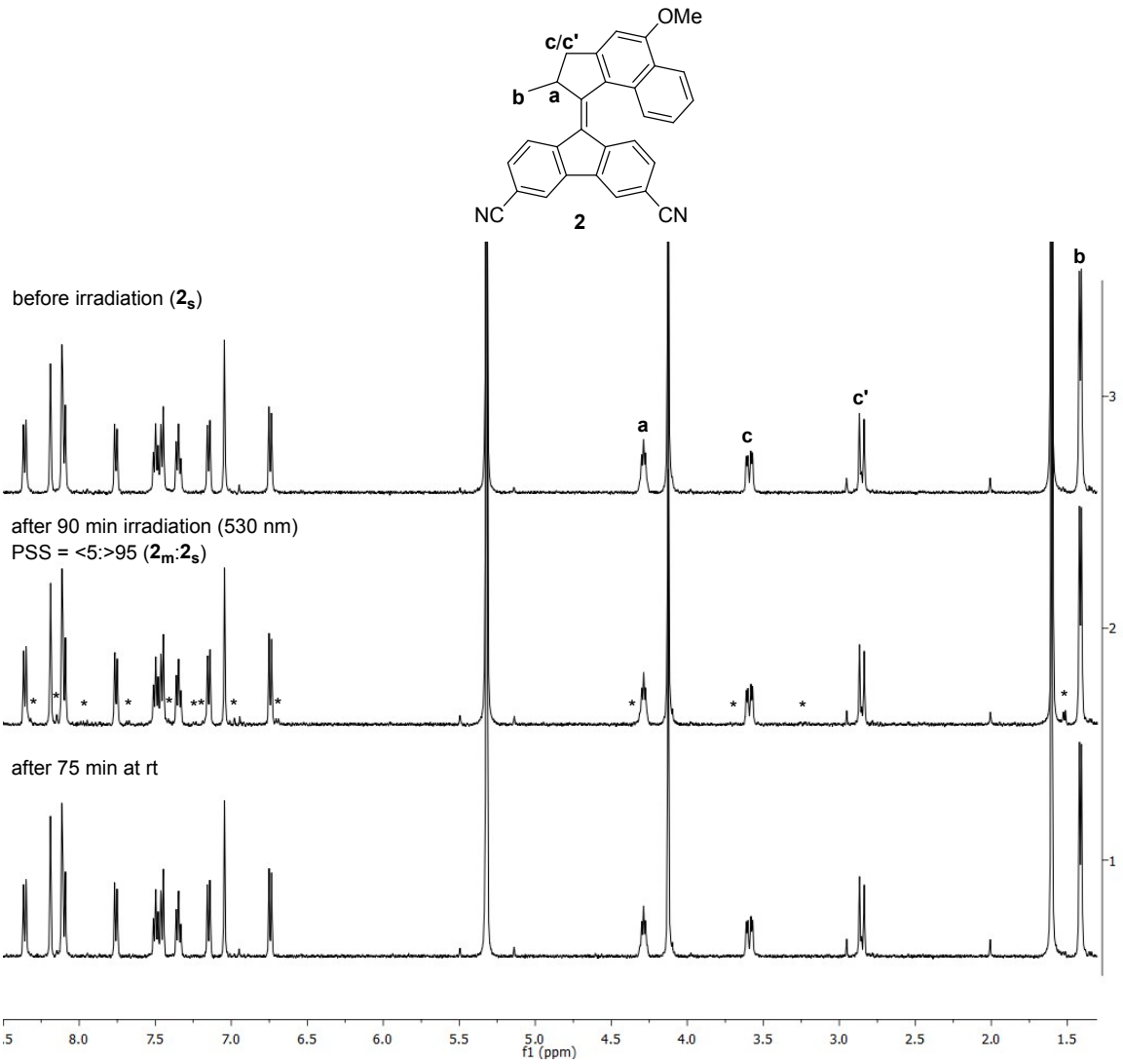

Figure S15. Stack of ^{1}H NMR spectra of **2** recorded at –10 °C before irradiation ($\mathbf{2}_s$), at PSS and after completed THI. Signals corresponding to $\mathbf{2}_m$ are marked with an asterisk (*).

Figure S16 shows the integration of the methyl signals (**b** in Figures S13 and S15) of $\mathbf{2}_s$ and $\mathbf{2}_m$ after irradiation with a 530 nm LED for 90 min.

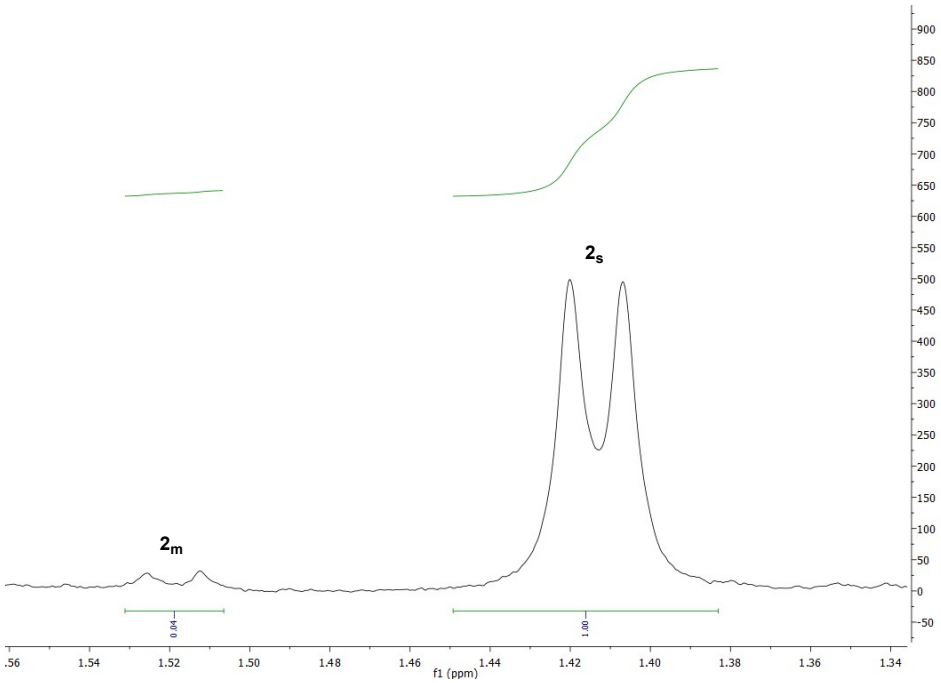

Figure S16. Zoom into ^{1}H NMR spectrum of PSS mixture of $\mathbf{2_s}$ and $\mathbf{2_m}$ recorded at –10 °C after irradiation with a 530 nm LED for 90 min.

Tables S9–S11 summarize the obtained PSS mixtures for motors **1**, **2** and **6** upon irradiation of samples of stable isomers with LEDs of different wavelengths.

Table S9. Ratios of $\mathbf{1_m}$:$\mathbf{1_s}$ at PSS after irradiation with LEDs of different wavelengths.

λ_{max} LED [nm]	$\mathbf{1_m}$:$\mathbf{1_s}$
420	74:26
455	50:50
470	25:75
490	<5:>95

Table S10. Ratios of $\mathbf{2_m}$:$\mathbf{2_s}$ at PSS after irradiation with LEDs of different wavelengths.

λ_{max} LED [nm]	$\mathbf{2_m}$:$\mathbf{2_s}$
455	76:24
470	63:37
490	32:68
505	24:76
530	<5:>95

Table S11. Ratios of $\mathbf{6_m}$:$\mathbf{6_s}$ at PSS after irradiation with LEDs of different wavelengths.

λ_{max} LED [nm]	$\mathbf{6_m}$:$\mathbf{6_s}$
420	88:12
455	63:37
470	34:66
490	<5:>95

6. Liquid Crystal Doping

6.1. Separation of Enantiomers

The enantiomers (*P*),(*R*)-**1**$_s$ and (*M*),(*S*)-**1**$_s$ for CD spectroscopy and LC doping/HTP determination experiments were isolated using supercritical fluid chromatography (SFC, Chiralpak IA, 60% CO_2 / 40% MeOH, 4.0 mL/min, T = 40 °C, 160 bar). A solution of racemic **1**$_s$ (10 mg/mL, $CHCl_3$) was prepared and 7 µL of this mixture were repeatedly loaded (60 consecutive injections, every 4.4 min) onto the column and the respective fractions were collected (Figure S17).

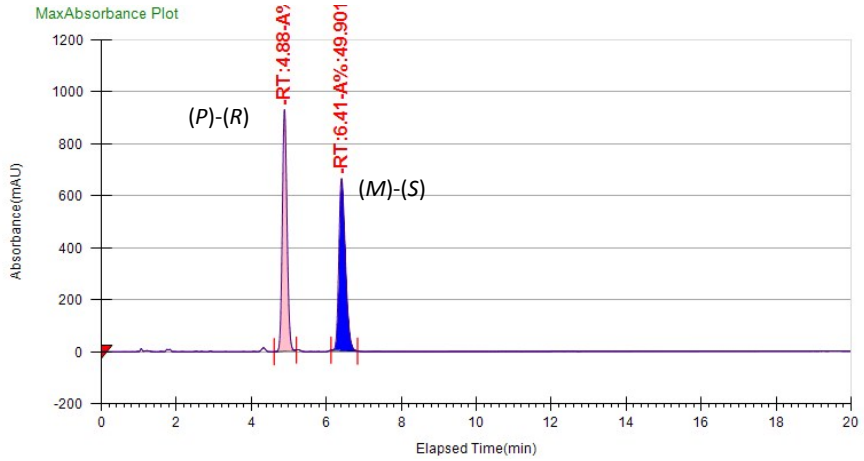

Figure S17. SFC (Chiralpak IA, 60% CO_2 / 40% MeOH, 4.0 mL/min, T = 40 °C, 160 bar) chromatogram of racemic **1**$_s$.

The enantiomers (*P*),(*R*)-**2**$_s$ and (*M*),(*S*)-**2**$_s$ for CD spectroscopy and LC doping/HTP determination experiments were isolated using SFC (Chiralpak ID, 60% CO_2 / 40% MeOH, 4.0 mL/min, T = 40 °C, 160 bar). A solution of racemic **2**$_s$ (10 mg/mL, $CHCl_3$) was prepared and 4 µL of this mixture were repeatedly loaded (50 consecutive injections, every 7.0 min) onto the column and the respective fractions were collected (Figure S18).

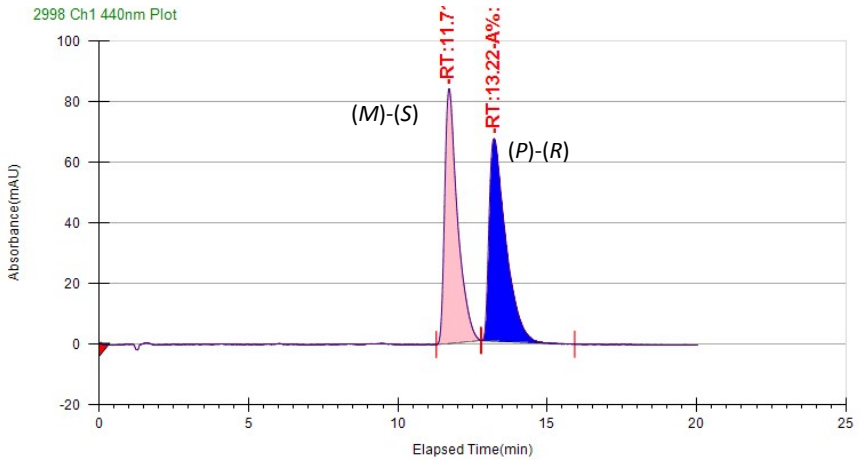

Figure S18. SFC (Chiralpak ID, 60% CO_2 / 40% MeOH, 4.0 mL/min, T = 40 °C, 160 bar) chromatogram of racemic **2**$_s$.

6.2. Assigning Enantiomers using Circular Dichroism (CD)

Solutions of both enantiomers of motors **1**$_s$ ($3.2\cdot10^{-5}$ M) and **2**$_s$ ($9.9\cdot10^{-6}$ M) in DCM were prepared and transferred into a 10 mm quartz cuvette. CD spectra were recorded at 20 °C before irradiation and after irradiation to PSS using a 420 nm (**1**$_s$) and 455 nm (**2**$_s$) LED, respectively. The obtained spectra for both enantiomers of the stable isomers before irradiation were compared with those predicted by DFT (TD-SCF DFT, CAM-B3LYP, 6-311G++(d,p)) to assign their respective handedness. Predicted CD spectra for stable isomers as well as experimental spectra before and after irradiation to PSS are shown in Figures S19–S22. Molar ellipticities (ϑ_M) for stable and metastable isomers at prominent wavelengths are summarised in Tables S12 and S13.

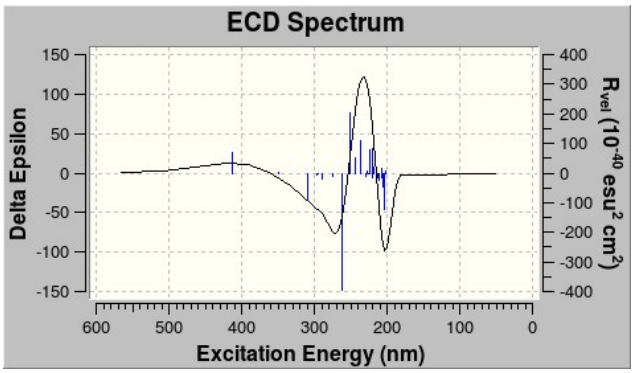

Figure S19. Calculated CD spectrum of (*M*),(*S*)-**1**$_s$ (TD-SCF DFT, CAM-B3LYP, 6-311G++(d,p)).

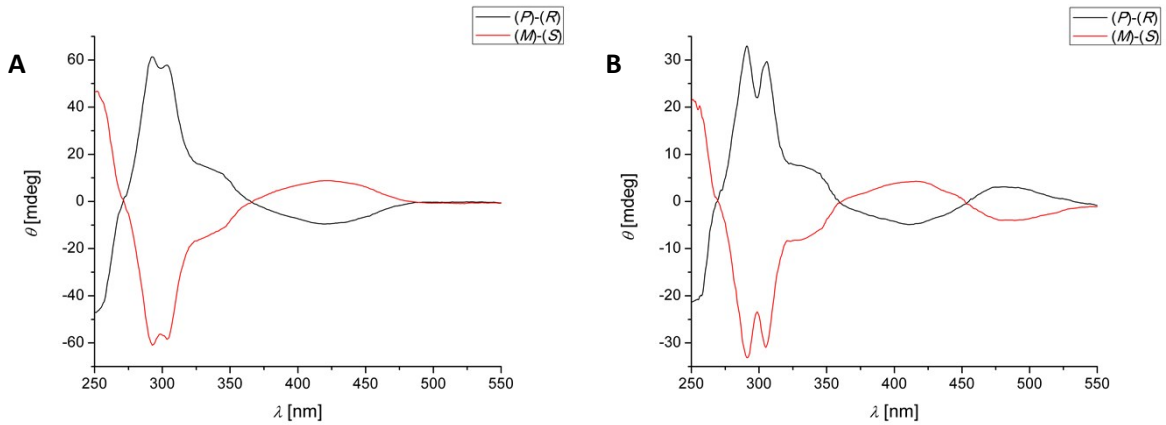

Figure S20. A: CD spectra of enantiomers of **1**$_s$. Conditions: DCM, 20 °C, $3.2\cdot10^{-5}$ M. **B**: CD spectra after irradiating to PSS. Conditions: 420 nm LED (0.50 A), 4 min.

Table S12. Molar ellipticities, ϑ_M, of **1**$_s$ and **1**$_m$ at characteristic wavelengths.

1$_s$		**1**$_m$	
λ [nm]	**ϑ_M [mdeg·M^{-1}·cm^{-1}]**	**λ [nm]**	**ϑ_M [mdeg·M^{-1}·cm^{-1}]**
293	$\pm1.67\cdot10^6$	291	$\pm6.41\cdot10^5$
304	$\pm1.57\cdot10^6$	306	$\pm5.64\cdot10^5$
350	$\pm2.33\cdot10^5$	350	$\pm6.09\cdot10^4$
422	$\pm2.57\cdot10^5$	411	$\pm9.37\cdot10^4$
		482	$\pm1.06\cdot10^5$

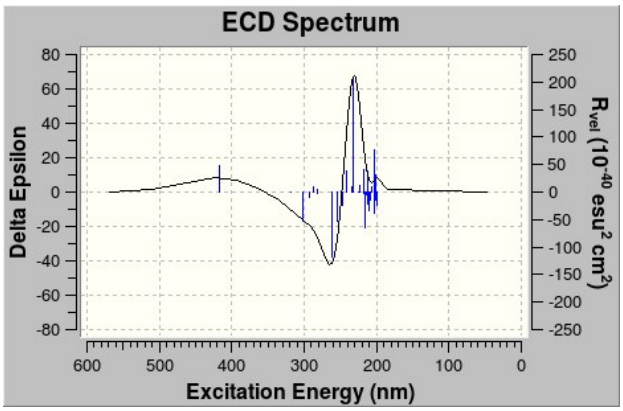

Figure S21. Calculated CD spectrum of (*M*),(*S*)-**2**$_s$ (TD-SCF DFT, CAM-B3LYP, 6-311G++(d,p)).

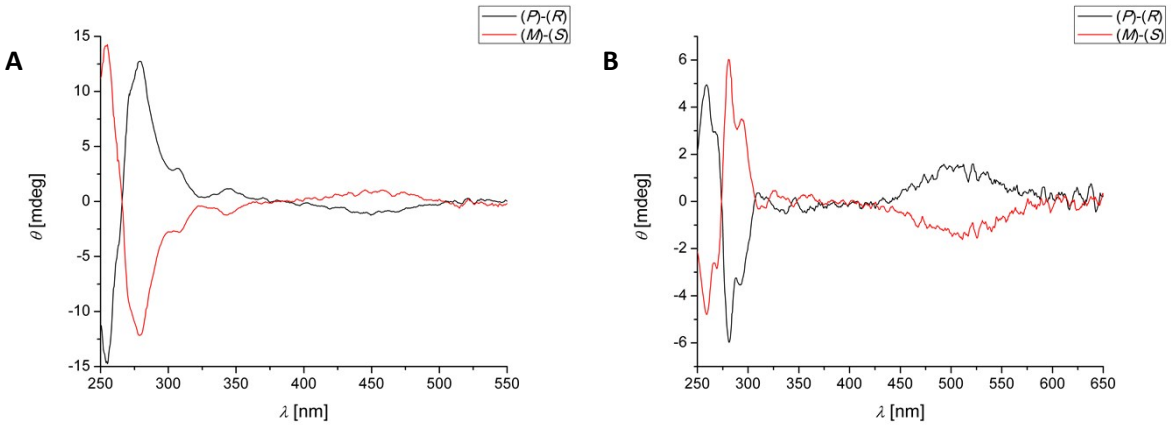

Figure S22. A: CD spectra of enantiomers of **2**$_s$. Conditions: DCM, 20 °C, 9.9·10^{-6} M. **B**: CD spectra after irradiating to PSS. Conditions: 455 nm LED (0.50 A), 4 min.

Table S13. Molar ellipticities, ϑ_M, of **2**$_s$ and **2**$_m$ at characteristic wavelengths.

2$_s$		**2**$_m$	
λ [nm]	**ϑ_M [mdeg·M^{-1}·cm^{-1}]**	**λ [nm]**	**ϑ_M [mdeg·M^{-1}·cm^{-1}]**
255	±1.50·10^6	259	±3.54·10^5
279	±1.29·10^6	269	±1.75·10^5
307	±3.05·10^5	281	±4.10·10^5
453[1]	±1·10^5	294	±3.25·10^5
		511[1]	±2·10^5

[1] Low accuracy due to noisy data.

6.3. Liquid Crystal Doping

The motor dopant was dissolved in DCM and mixed with E7 (dopant concentration ca. 1 *wt*%). The solvent was then evaporated under a N_2 stream and the remaining mixture was heated up to 60 °C. After stirring at 60 °C for 30 min it was allowed to cool to room temperature and the mixture was capillary-filled into a wedge cell (KCRK-03 with a wedge angle of 0.45° (tan ϑ = 0.0078). The mixture in the wedge cell was heated up to 60 °C and then allowed to slowly cool down to 25 °C at a rate of 1 °C/min For irradiation of motors **1**$_s$ and **2**$_s$ a 420 nm and 455 nm LED (1.0 mW) was used, respectively.

The light source was held at an angle of 60° with respect to the sample plane, to allow irradiation under the microscope.

Helical twisting powers were determined using the Grandjean-Cano method.[14] The helical pitch (p) is thereby calculated from the measured distance between the Cano lines in the sample (R) and the cell angle (α) according to Eq. 8.

$$\frac{p}{2} = R * tan(\alpha) \qquad \text{Eq. 8}$$

From this the helical twisting power (β) can be obtained using the concentration of dopant (c) and its *ee* according to Eq. 9.

$$\beta = \frac{1}{p * c * ee} \qquad \text{Eq. 9}$$

Figure S23 shows examples of the pitch change observed in a wedge cell before and after irradiating motor **1**$_s$ (420 nm LED, 1.0 mW) to PSS.

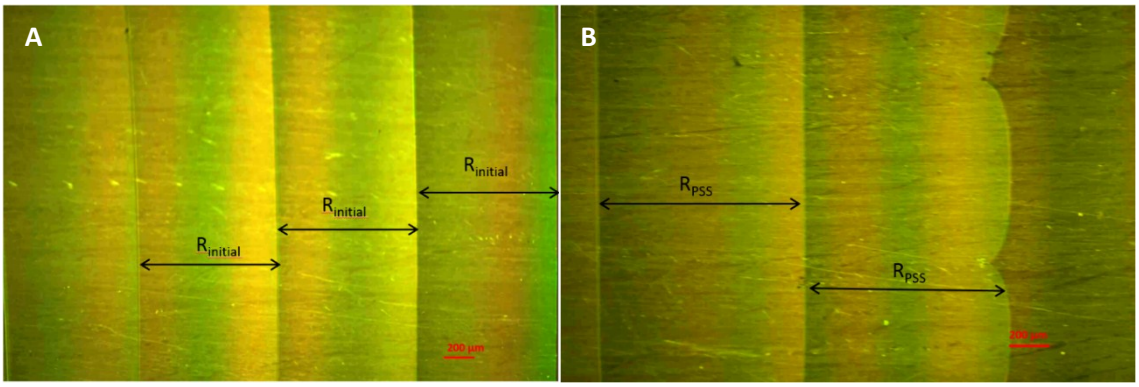

Figure S23. A: Cano wedge cell images with Cano lines (scale bar 200 µm) obtained from cholesterid E7 liquid crystals doped with ca. 1 wt% of **1**$_s$ before and after irradiation to PSS using a 420 nm LED (1.0 mW).

7. References

[1] M. M. Pollard, P. V. Wesenhagen, D. Pijper and B. L. Feringa, *Org. Biomol. Chem.,* 2008, **6**, 1605–1612.

[2] J. Conyard, P. Štacko, J. Chen, S. McDonagh, C. R. Hall, S. P. Laptenok, W. R. Browne, B. L. Feringa and S. R. Meech, *J. Phys. Chem. A*, 2017, **121**, 2138–2150.

[3] D. D. Hennings, T. Iwama and V. H. Rawal, *Org. Lett.*, 1999, **1**, 1205–1208.

[4] M. Valášek, K. Edelmann, L. Gerhard, O. Fuhr, M. Lukas and M. Mayor, *J. Org. Chem.*, 2014, **79**, 7342–7357.

[5] J.-H. Fournier, T. Maris and J. D. Wuest, *J. Org. Chem.*, 2004, **69**, 1762–1775.

[6] C. Chuang, S. C. Lapin, A. K. Schrock and G. B. Schuster, *J. Am. Chem. Soc.* 1985, **107**, 4238–4243.

[7] W. Chew, R. Hynes and D. N. Harpp, *J. Org. Chem.* 1993, **58**, 4398–4404.

[8] M. J. Frisch, G. W. Trucks, H. B. Schlegel, G. E. Scuseria, M. A. Robb, J. R. Cheeseman, G. Scalmani, V. Barone, G. A. Petersson, H. Nakatsuji, X. Li, M. Caricato, A. V. Marenich, J. Bloino, B. G. Janesko, R. Gomperts, B. Mennucci, H. P. Hratchian, J. V. Ortiz, A. F. Izmaylov, J. L. Sonnenberg, D. Williams-Young,

F. Ding, F. Lipparini, F. Egidi, J. Goings, B. Peng, A. Petrone, T. Henderson, D. Ranasinghe, V. G. Zakrzewski, J. Gao, N. Rega, G. Zheng, W. Liang, M. Hada, M. Ehara, K. Toyota, R. Fukuda, J. Hasegawa, M. Ishida, T. Nakajima, Y. Honda, O. Kitao, H. Nakai, T. Vreven, K. Throssell, J. A. Montgomery Jr., J. E. Peralta, F. Ogliaro, M. J. Bearpark, J. J. Heyd, E. N. Brothers, K. N. Kudin, V. N. Staroverov, T. A. Keith, R. Kobayashi, J. Normand, K. Raghavachari, A. P. Rendell, J. C. Burant, S. S. Iyengar, J. Tomasi, M. Cossi, J. M. Millam, M. Klene, C. Adamo, R. Cammi, J. W. Ochterski, R. L. Martin, K. Morokuma, O. Farkas, J. B. Foresman and D. J. Fox, *Gaussian 16*, *Revision B.01*, Gaussian Inc., Wallingford CT, 2016.

[9] R. Dennington, T. Keith and J. Millam, *Gauss View*, *Version 5*, Semichem Inc., Shawnee Mission, 2009.

[10] W. L. DeLano, *The PyMOL Molecular Graphics System*, DeLano Scientific LLC, San Carlos CA, 2002.

[11] H. J. C. Berendsen, D. van der Spoel and R. van Drunen, *Comp. Phys. Comm.*, 1995, **91**, 43–56.

[12] E. Lindahl, B. Hess and D. van der Spoel, *J. Mol. Mod.*, 2001, **7**, 306-317.

[13] M. Montalti, A. Credi, L. Prodi and M. T. Gandolfi, *Handbook of Photochemistry*, 3rd Edition, CRC Press, 2006.

[14] I. Dierking, *Textures of Liquid Crystals*, Miley-VCH, Weinheim, 2003.

8. NMR Spectra

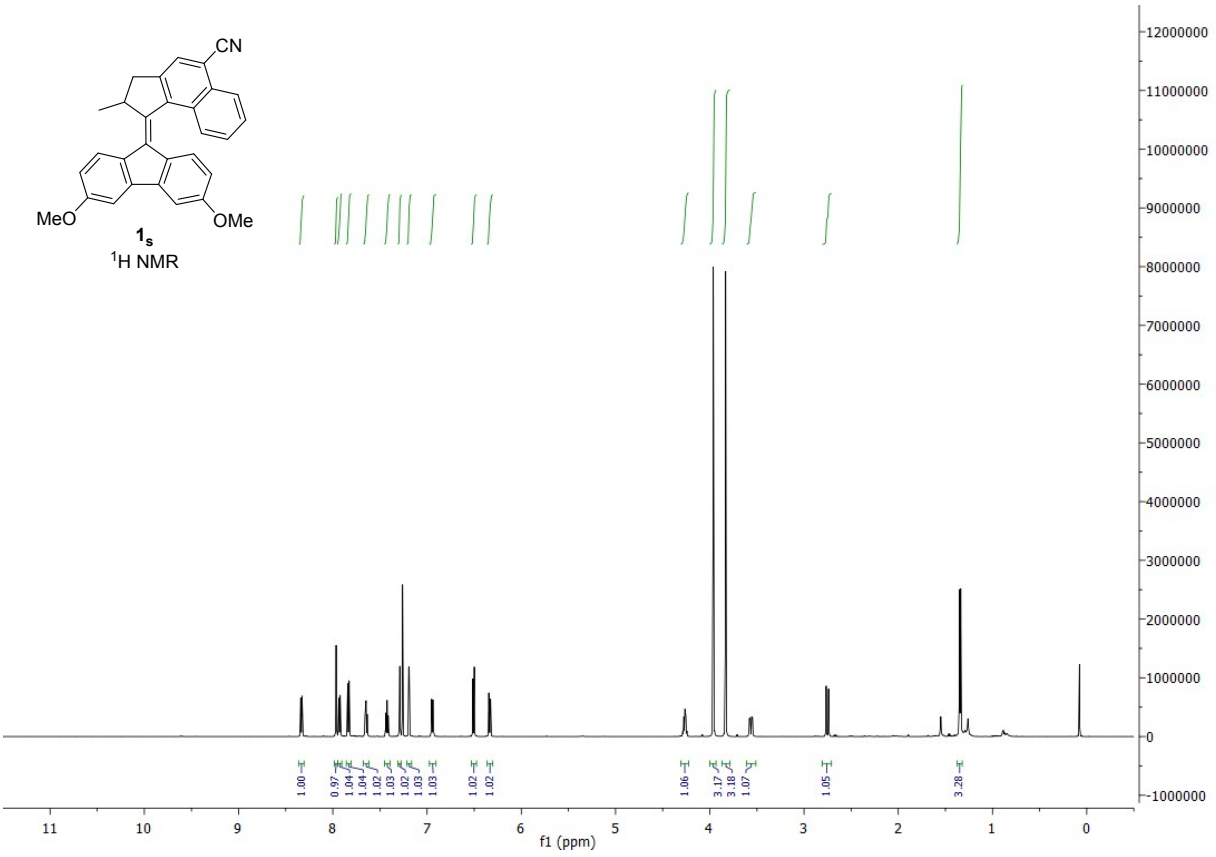

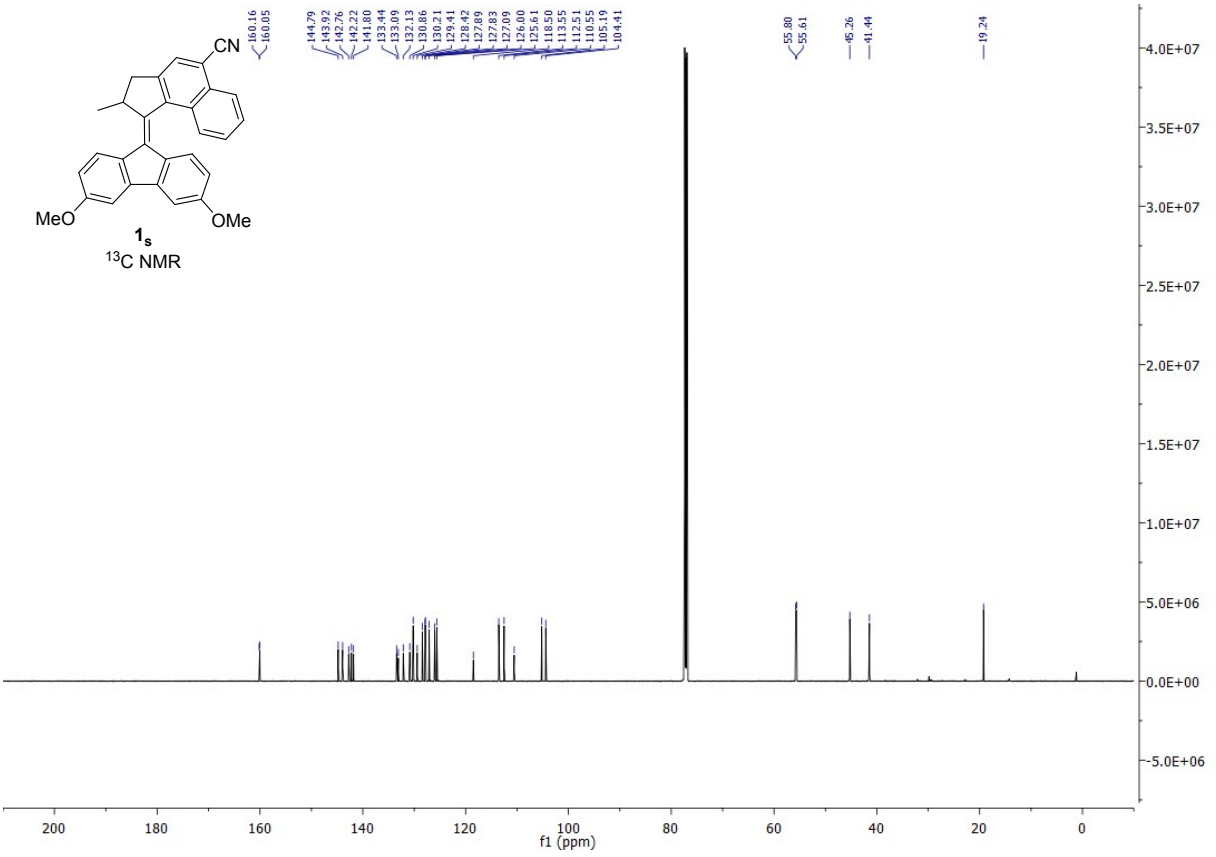

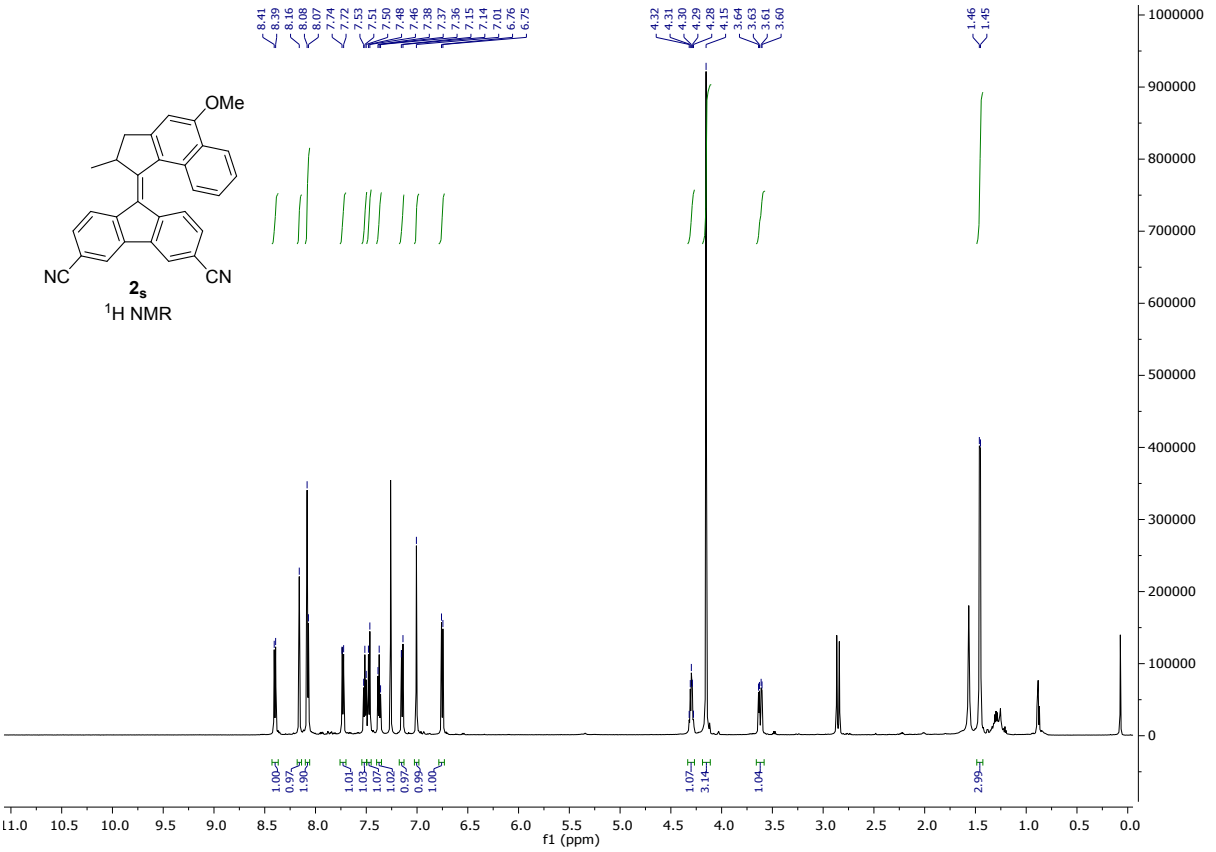
OMe
NC
CN
2s
1H NMR
f1 (ppm)

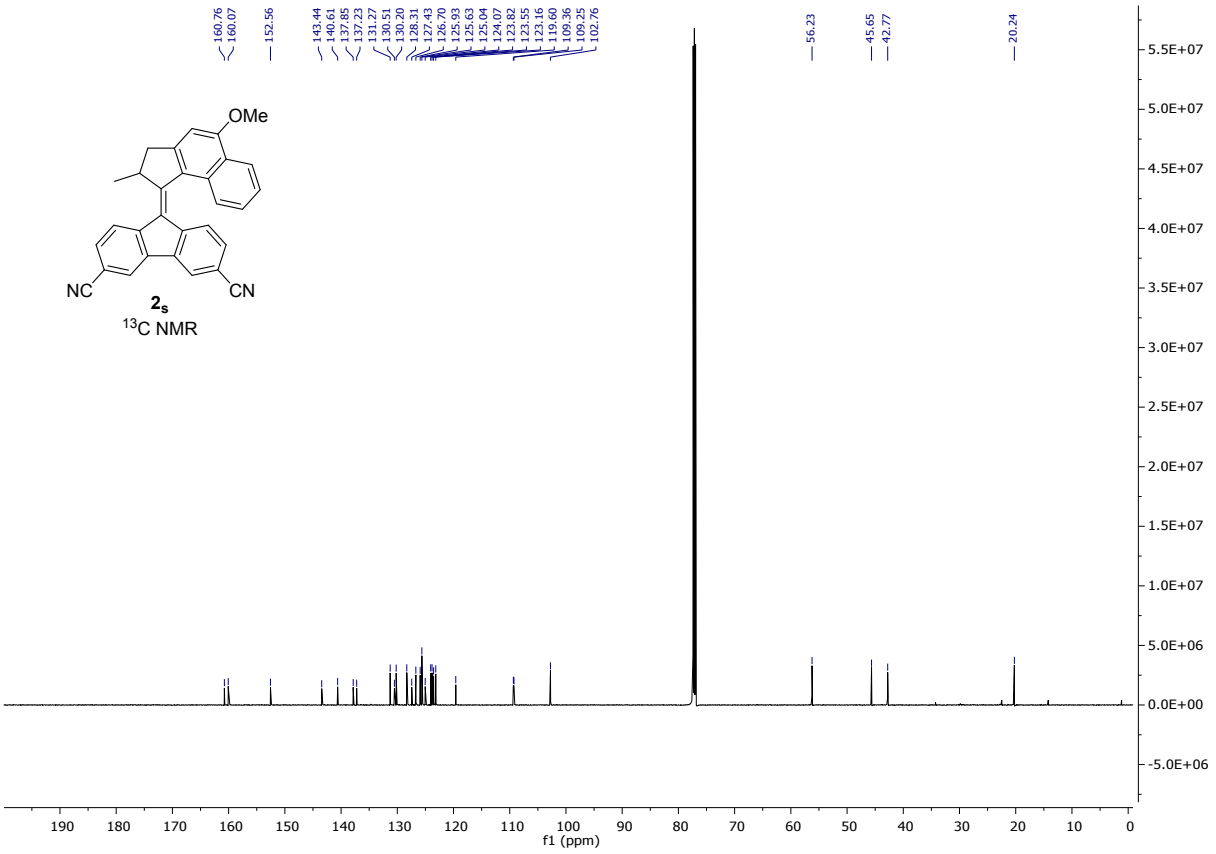
OMe
NC
CN
2s
13C NMR
f1 (ppm)

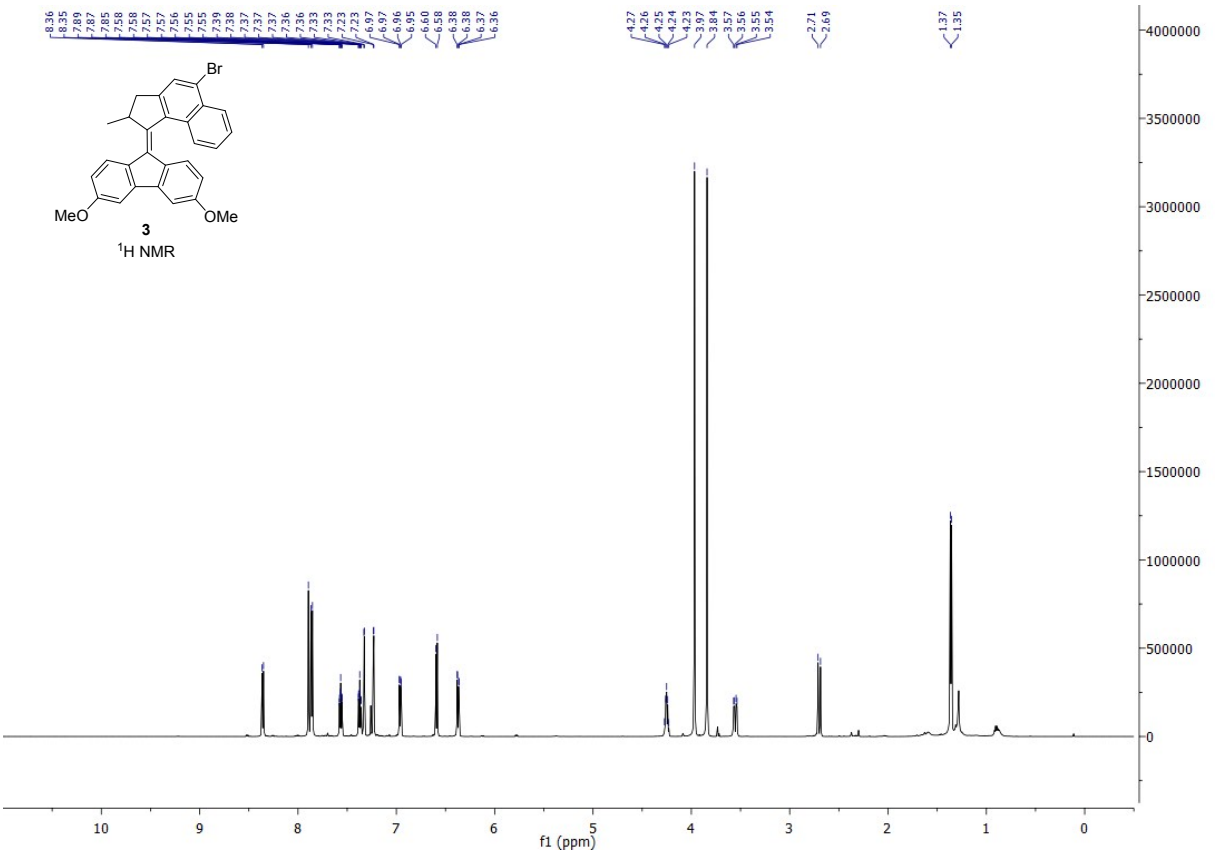
Br
MeO
OMe
3
1H NMR
f1 (ppm)

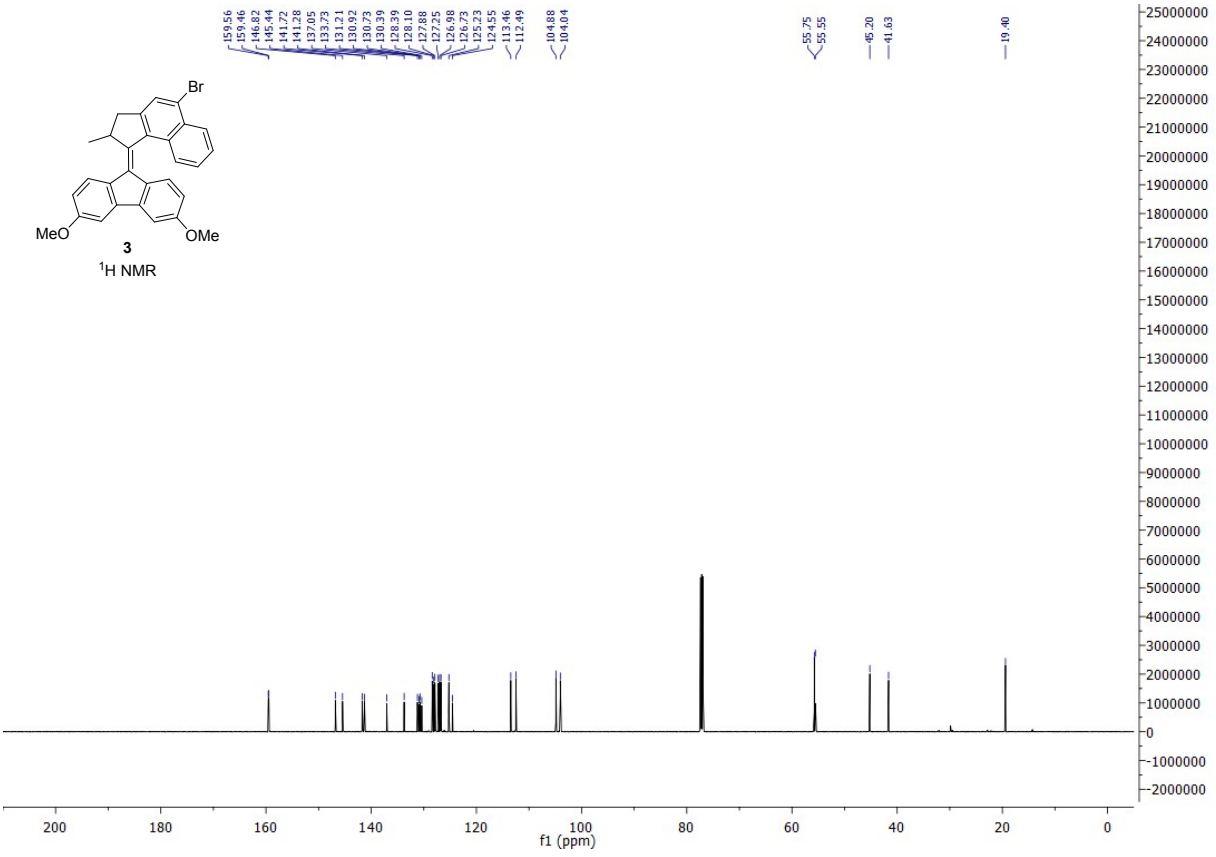
Br
MeO
OMe
3
1H NMR
f1 (ppm)

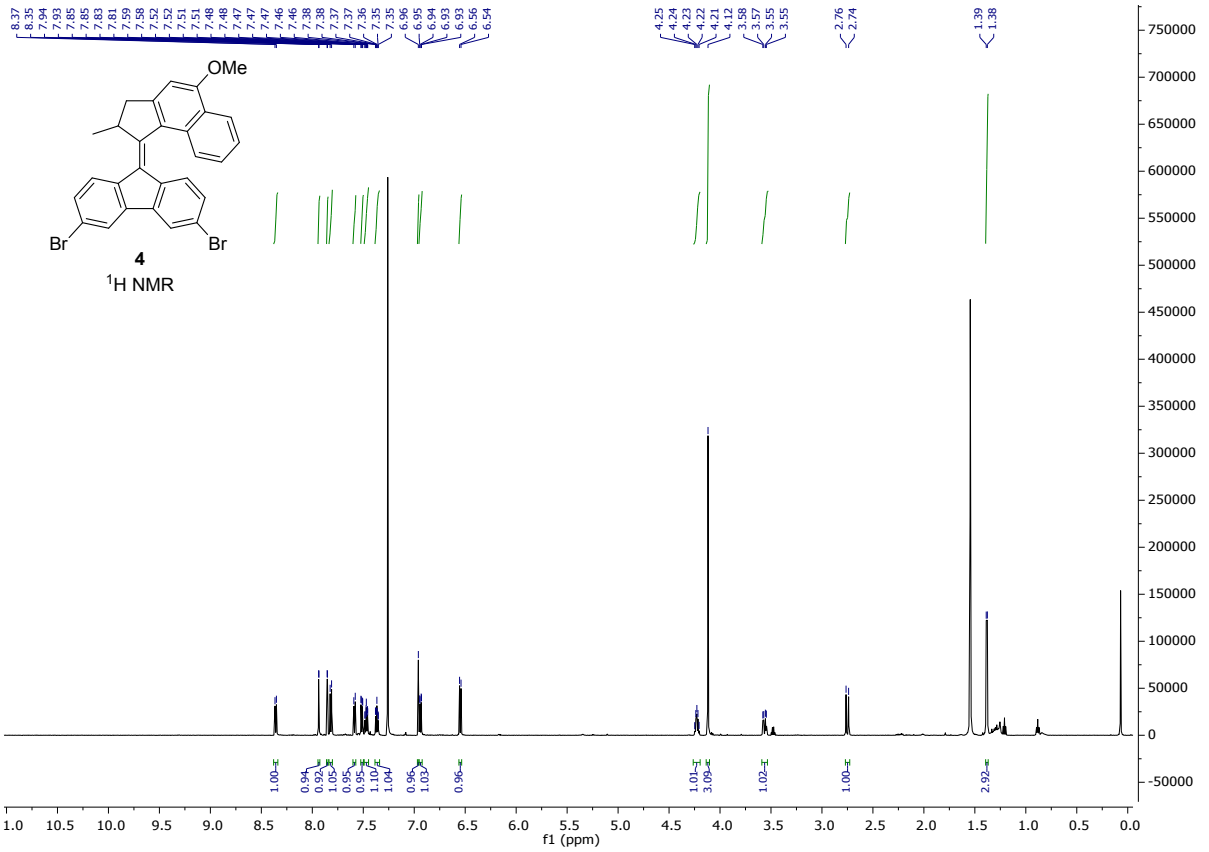
OMe
Br
Br
4
1H NMR
f1 (ppm)

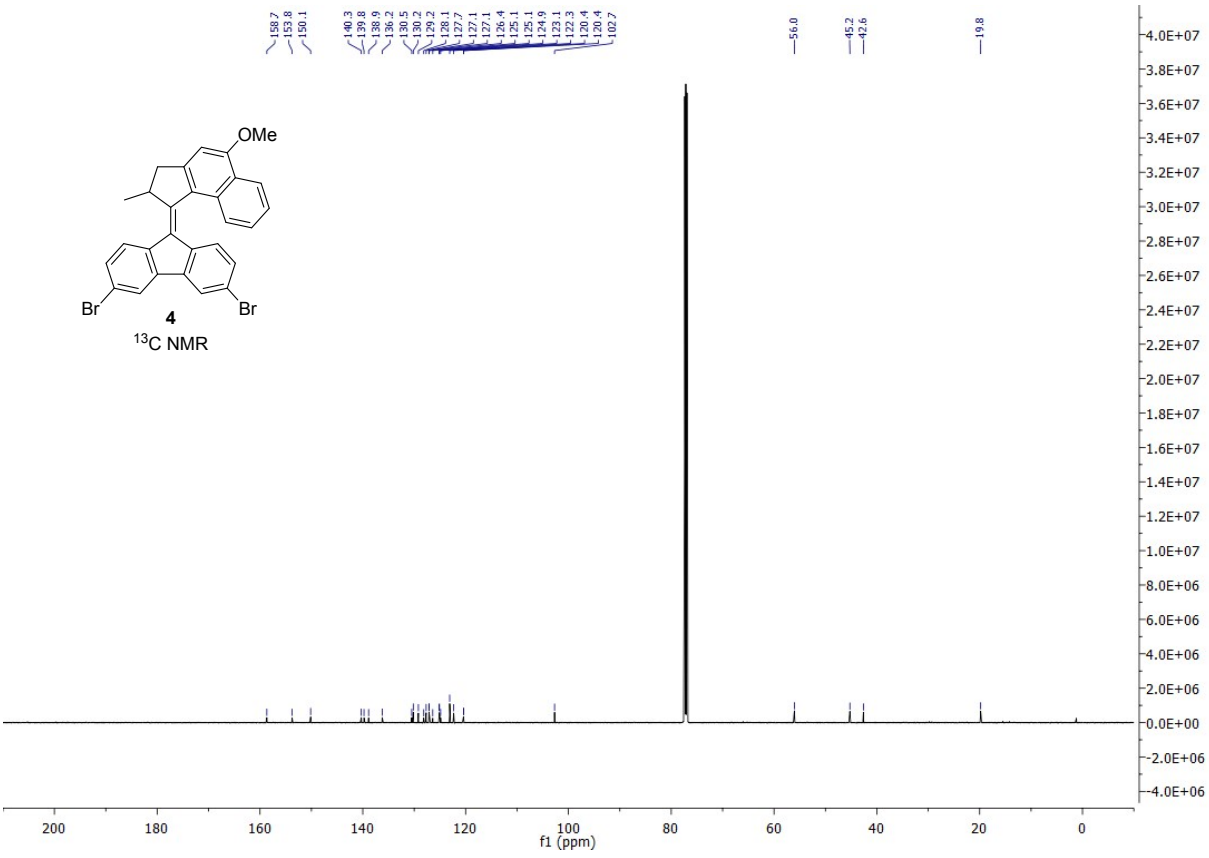
OMe
Br
Br
4
13C NMR
f1 (ppm)

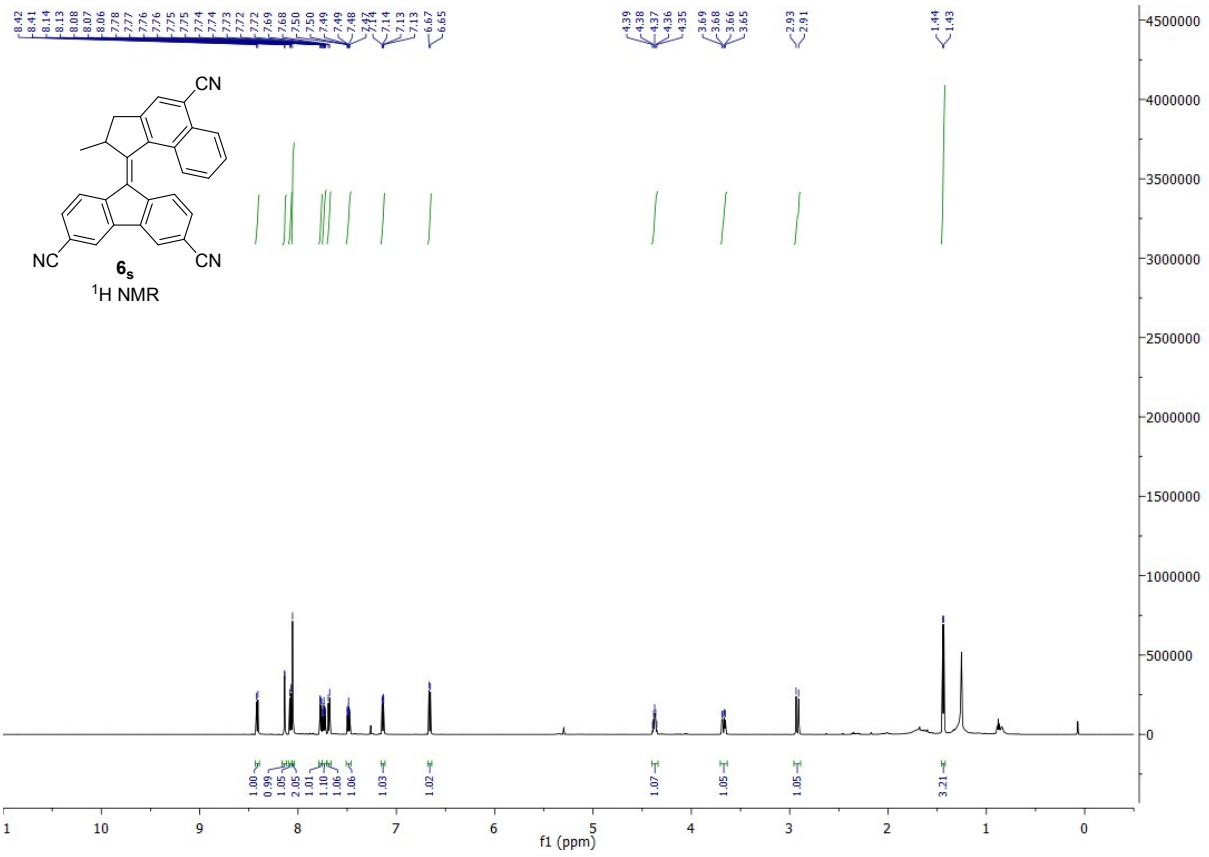
CN
NC
CN
6s
1H NMR
f1 (ppm)

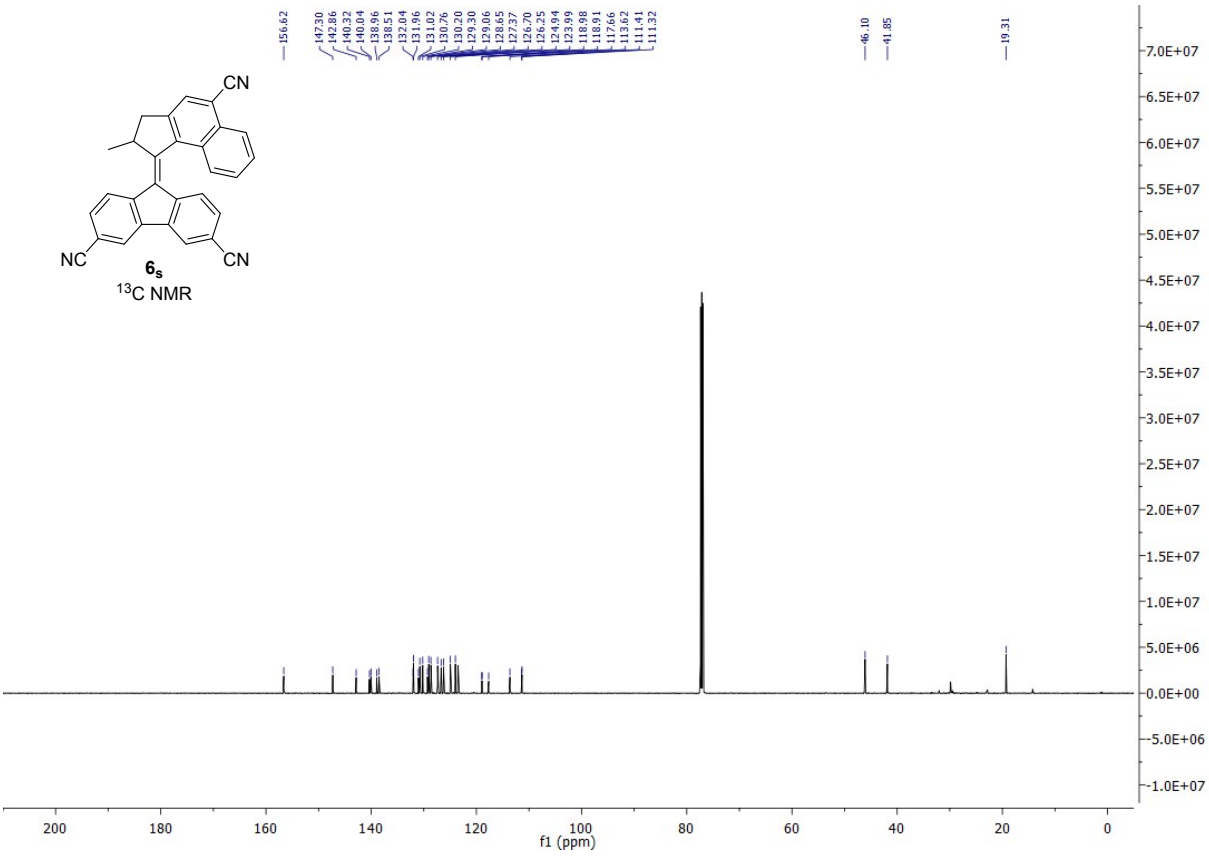
CN
NC
CN
6s
13C NMR
f1 (ppm)